NTNU – Trondheim
Norwegian University of
Science and Technology

SCOUR BELOW PIPELINES AND AROUND VERTICAL PILES DUE TO RANDOM WAVES PLUS CURRENT ON MILD SLOPES

Ping Fu

Marine Technology
Submission date: June 2014
Supervisor: Dag Myrhaug, IMT

Norwegian University of Science and Technology
Department of Marine Technology

I would like to dedicate this thesis to my loving parents.

NTNU Trondheim
Norwegian University of Science and Technology
Department of Marine Technology – Group of Marine Structures

MASTER THESIS IN MARINE TECHNOLOGY

SPRING 2014

FOR

STUD. TECHN. PING FU

SCOUR BELOW PIPELINES AND AROUND VERTICAL PILES DUE TO RANDOM WAVES PLUS CURRENT ON MILD SLOPES

Pipelines and vertical piles on sloped sandy seabeds in the coastal zone are exposed to random waves plus current, and consequently scour close to the structures will develop. The assessment of scour below pipelines and around vertical piles is essential in design of the structures and in scour protection work.

This thesis will focus on combining the use of the Sumer and Fredsøe (2002) flat bed scour formulas for pipelines and vertical piles and the Battjes and Groenendijk (2000) wave height distribution for mild slopes.

The student shall:

1. Give an overview of the scour mechanisms below marine pipelines and around vertical piles.
2. Give the background of scour around marine pipelines and vertical piles on flat and sloping seabeds for regular and random waves without and with a current.
3. Give a brief description of the Battjes and Groenendijk (2000) wave height distribution for mild slopes.
4. Apply the scour formulas on a flat bed described in Part 2 together with the wave height distribution over mild slopes.
5. Both stochastic and approximate method results shall be presented and discussed.

The work scope may prove to be larger than initially anticipated. Subject to approval from the supervisor, topics may be deleted from the list above or reduced in extent.

In the thesis the candidate shall present her personal contribution to the resolution of problem within the scope of the thesis work.

Theories and conclusions should be based on mathematical derivations and/or logic reasoning identifying the various steps in the deduction.

The candidate should utilize the existing possibilities for obtaining relevant literature.

The thesis should be organized in a rational manner to give a clear exposition of results, assessments, and conclusions. The text should be brief and to the point, with a clear language. Telegraphic language should be avoided.

The thesis shall contain the following elements: A text defining the scope, preface, list of contents, summary, main body of thesis, conclusions with recommendations for further work, list of symbols and acronyms, reference and (optional) appendices. All figures, tables and equations shall be numerated.

The supervisor may require that the candidate, in an early stage of the work, present a written plan for the completion of the work. The plan should include a budget for the use of computer and laboratory resources that will be charged to the department. Overruns shall be reported to the supervisor.

The original contribution of the candidate and material taken from other sources shall be clearly defined. Work from other sources shall be properly referenced using an acknowledged referencing system.

The thesis shall be submitted:

- Signed by the candidate
- The text defining the scope included
- In bound volume(s)
- Drawings and/or computer prints which cannot be bound should be organized in a separate folder.
-

Advisors: Dr. Muk Chen Ong, Marintek
Professor Dag Myrhaug

Deadline: 10.06.2014

Dag Myrhaug
Supervisor

Acknowledgements

This thesis has been written as a part of the Master degree in Department of Marine Technology at Norwegian University of Science and Technology (NTNU) during the spring semester of 2014. This work has been strongly motivated by personal interest in waves and current, stochastic theory of sealoads and oceanography.

The paper is prepared in LaTeX, and the numerical analysis and the generation of figures are performed in Matlab.

I would like to thank my supervisor, Prof. Dag Myrhaug. He, with his deep understanding of scour, and his kind and patient personality, helped me a lot during this study. Thanks for his instruction, insight, and inspiration. I learned from him, what does it mean to be a good researcher.

I further want to thank my co-supervisor Dr. Muk Chen Ong for all the details and discussions we had on my thesis. He has set a good example for me by his enthusiasm to research. His contributions to this work are highly appreciated.

This thesis ends two years of studies at NTNU. The experience and the knowledge acquired during this period is very important. Many people helped me to achieve my target. I am grateful to my parents for their constant support and kindness. I am thankful to my husband, who stands besides me and supports me with his patience and understanding during all two years .

Finally, I address a special thanks to all my friends in Trondheim. Thanks for all the time we spent together.

Abstract

This thesis presents a stochastic method for predicting the scour depth around vertical circular slender piles and below marine pipelines due to random waves plus current on mild sloping seabeds. An overview of the scour mechanisms around vertical piles and below marine pipelines is given. The background of the scour around vertical piles and below marine pipelines on flat and sloping seabeds under regular waves and random waves alone, as well as random waves plus current is presented.

A point model of the wave height distribution, consisting of two two-parameter Weibull distribution, is chosen to describe the wave condition on mild sloping seabeds including breaking waves. For vertical piles, a truncated wave height distribution is developed because the scour formula is valid above a threshold value.

Four slopes are considered for waves alone case for the vertical piles and the pipelines. The effect of combined waves plus current on scour is studied. For waves plus current, the relationship between scour depth and the current velocity is presented. A comparison between a stochastic method and an approximate method is made.

Contents

List of Figures

List of Tables

Nomenclature

Roman Symbols

(c, d)	Coefficients for calculating the friction factor
(C, q, r)	Coefficients for calculating pile scour
α	Shear stress amplification factor
δ	Bed boundary layer thickness
$\hat{H}_{1/n}$	Value of $\hat{H}$ exceeded with a probability of $1/n$
$\hat{H}$	Normalized wave height
$\hat{H}_t$	Truncation point of wave height distribution
$\hat{H}_{tr}$	Transitional wave height
$\hat{S}_{1/n}$	Scour caused by $(1/n)th$ highest waves
$\hat{S}_{cw1/n}$	Scour caused by $(1/n)th$ highest waves plus current
$\hat{U}_m$	Dimensionless maximum horizontal fluid velocity at the seabed
ν	Kinematic viscosity of flow
ω	Angular wave frequency
ω_p	Peak frequency
ϕ	Angle between current and waves
ρ	Density of water
ρ_s	Sediment density

τ	Shear stress
τ_∞	Undisturbed shear stress
θ	Shields parameter
θ_{cr}	Critical value of Shields parameter
$\zeta(t)$	Free surface elevation
A	Linear near-bed orbital velocity amplitude
$a(t)$	Time-dependent near-bed orbital displacement
D	Characteristic diameter
d_{50}	Median grain diameter
e	Gap between seabed and pipe
$E[A_{1/n}]$	Alternative A defined in the approximate method
$E[U_{1/n}]$	Alternative U defined in the approximate method
F	Non-dimensional parameter utilized for pipeline scour
f_w	Friction factor
g	Acceleration of gravity
H	Linear wave height
h	Water depth
$H_{1/n}$	Value of H exceeded with a probability of $1/n$
H_{m_0}	Significant wave height
k	Wave number
k_p	Wave number corresponding to ω_p
KC	Keulegan-Carpenter number
$KC_{1/n}$	Alternative KC number defined in the approximate method

KC_{rms}	Root-mean-square value of the Keulegan-Carpenter number
L	Horizontal length of the sloping seabeds
m_0	Zeroth spectrum moment
$P(\hat{H})$	Cumulative distribution function of $\hat{H}$ (cdf)
$p(\hat{H})$	Probability density function of $\hat{H}$ (pdf)
$R_{1/n}$	Ratio between the stochastic and the approximated method for waves alone case
$R_{cw1/n}$	Ratio between the stochastic and the approximated method for waves plus current case
R_{e_d}	Pile Reynolds number
S	Equilibrium scour depth
s	Ratio between ρ_s and ρ
S_t	Instantaneous scour depth
$S_{\zeta\zeta}(\omega)$	Wave spectrum in deep water
$S_{\zeta\zeta}(\omega,\ h)$	Wave spectrum in finite water depth
S_{cur}	Scour depth for pipeline in current alone
T	Wave period
t	Time
T_p	Peak period of the wave spectrum
U	Linear near-bed orbital displacement amplitude
$u(t)$	Time-dependent near-bed orbital velocity
U_c	Current velocity
U_m	Undisturbed linear near-bed orbital velocity amplitude
U_{cwrms}	Coefficient based on U_c and U_{rms}

U_{cw}	Coefficient based on U_c and U
U_{rms}	Root-mean-square value of U
z_0	Bed roughness

Chapter 1

Introduction

When a structure is placed the sandy seabed, the presence of the structure will change the incoming flow. The changed flow transports sand particles away from the structure, creating a hole around it. This phenomenon is called scour. The scour is a threat to the stability of marine structures, such as vertical piles (foundations of offshore wind turbines) or marine pipelines. For vertical pipes, the scour increases the over-length of the pipe, further lowering the natural frequency and probably leading to structural failure. For marine pipelines, scour may expose part of the pipeline, leading it to be suspended or partially buried. If the free span is long enough, the pipeline may experience flow-induced oscillations, resulting in structural failure. The results of scour depend on the geometry and material of the seabeds, the velocity of the incoming flow and ratio between the orbital fluid particle displacement and the characteristic dimension of the structure.

The flow can be considered as a steady current in deep water, while in finite water depth, it is commonly combined waves plus current. Scour in a steady current has been studied extensively. Kjeldsen et al. (1973) were the first to conduct scour experiments and presented data on the maximum scour depth below pipelines at a fixed location. Those results suggested the relationship between scour depth and the Shields parameter (defined in Chapter 2) in a current. Sumer and Fredsøe (1990) investigated the scour below pipelines exposed to regular waves. They found the scour in this case weakly varies with the Shields parameter, but strongly depends on KC number (defined in chapter 4). Further they proposed an empirical formula for scour below pipelines in regular waves. The corresponding formula for vertical piles was presented in Sumer et al. (1992a). The influence of cross section shape of the pipes was investigated through laboratory experiments by Sumer et al. (1993). For random waves, Sumer and Fredsøe (1996) conducted experiments and gave the empirical formulas for scour depth below pipelines in random waves and combined random waves

plus current, respectively. The corresponding formulas for vertical piles were proposed by Sumer and Fredsøe (2001).

In real life, waves are of stochastic nature, which makes the problem more complicated. Myrhaug and Rue (2003) presented a stochastic method for evaluation of the scour depth below pipelines and around vertical piles in random waves on a flat seabed based on Sumer and Fredsøe (1996, 2001) scour formulas. They assumed that the sea state is a stationary narrow-band process and compared their results with the Sumer and Fredsøe (1996, 2001) random waves data. Further, this approach was expanded by Myrhaug et al. (2009) to apply on scour around marine structures due to second-order random waves plus current for wave-dominant flow. Comparisons were also made with the data from Sumer and Fredsøe (2000) for liner waves. Moreover, This stochastic method for scour depth assessment has been extended to other marine structures: a group of pipes in random waves,(Myrhaug and Rue (2005)); a spherical body (Myrhaug and Ong (2012)); a short cylinder (Myrhaug and Ong (2009)) and truncated cones (Myrhaug and Ong (2014)).

For shoaling conditions, Cevik and Yüksel (1999) investigated the scour for sloping beds with two beach slopes, 1/5 and 1/100. They obtained an empirical formula for scour depth in such a shoaling condition by laboratory tests. By utilizing this formula, Myrhaug et al. (2008) presented the stochastic method for evaluating scour below pipelines in random waves in coastal regions. Further, Henry and Myrhaug (2013) extended this approach on shoaling condition to calculate wave-induced drag force on vegetation under shoaling random waves. To author's knowledge, no studies, except for the master project of Ping (2013), are yet available in the open literature dealing with scour around marine structures exposed to random waves and combined random waves plus current on sloping seabeds by stochastic method.

The purpose of this study is to provide a stochastic method for estimating the scour depth around vertical piles and below pipelines due to random waves plus current on mild sloping seabeds. This is achieved by using the Sumer and Fredsøe (1996, 2001) scour formulas on flat seabeds, combined with the Battjes and Groenendijk (2000) wave height distribution for mild slopes including the effect of breaking waves. It should be noted that the wave motion is assumed as a stationary narrow-band random process. Results for waves alone and waves plus current are presented and discussed. An approximated method was proposed and compared with the present stochastic method.

Chapter 2

Background

2.1 Seabed shear stress

The presence of a structure in marine environment will change the flow pattern around it. Generally, these changes cause an increase of the bed shear stress and the level of turbulence close to the structure. As a result, the local sediment transport capacity increases, leading to scour. Usually, the increase of the bed shear stress is expressed by the amplification factor α, defined as (Sumer and Fredsøe (2002))

$$\alpha = \frac{\tau}{\tau_\infty} \tag{2.1}$$

where, τ is the bed shear stress around structures and τ_∞ is the bed shear stress for the undisturbed flow. Due to the local increase in α, the sediment transport capacity will increase, leading to the scour process. This process will continue until this process reaches a stage where the bed shear stress around structures $\tau = \tau_\infty$ ($\alpha = O(1)$). This stage where the scour process come to the end is called the equilibrium stage. The corresponding scour depth is called the equilibrium scour depth. The time it takes to develop the equilibrium scour, as illustrated in Fig. 2.1, is called the time scale of the scour process and defined as (Sumer and Fredsøe (2002))

$$S_t = S\left(1 - \exp\left(\frac{t}{T}\right)\right) \tag{2.2}$$

where S is the equilibrium scour depth corresponding to the equilibrium stage, and S_t is the instantaneous scour depth at time t. The equilibrium scour depth is of great importance for indicating the degree of scour potential. The time scale is an equally important parameter because scour often occurs during storms. It is essential to assess whether the storm would

long enough to develop a substantial amount of scour.

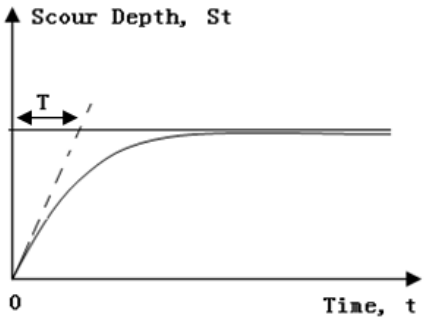

Fig. 2.1 Time development of scour depth (reproduced from Sumer and Fredsøe (2002)).

2.2 Shields parameter

Typically, there are two scour categories: the clear-water scour and the live-bed scour. The category can be determined by judging the Shields parameter θ, defined as

$$\theta = \frac{\tau_\infty}{\rho g(s-1)d_{50}} \tag{2.3}$$

where $s = \rho_s/\rho$ is the sediment density to fluid density ratio, ρ_s is the sediment density and ρ is the fluid density. g is the gravity acceleration and d_{50} is the median grain size of the sediments. It should be noted that τ_∞ should be replaced by the maximum value of undisturbed shear stress $\tau_{\infty,max}$ in waves. For the clear-water scour, the sediment transport is localized, that means no sediment motion takes place far from the structure ($\theta < \theta_{cr}$), while for the live-bed scour, sediment transport prevails over the entire sea bed ($\theta > \theta_{cr}$). θ_{cr} is the critical value for the onset of motion of sediment.

When the seabed is sloping, the effect of gravity of the sediments may increase or decrease θ_{cr}. Thus, the threshold shear stress at an up-sloping seabed with an angle δ , denoted as $\theta_{\delta cr}$, can be expressed by modifying the corresponding critical value at horizontal seabed

$$\frac{\theta_{\delta cr}}{\theta_{cr}} = \cos\delta(1 + \frac{\tan\delta}{\tan\Phi_i}) \tag{2.4}$$

where Φ_i is the angle of repose of the sediment.

The maximum bed shear stress within a wave cycle is given as

$$\frac{\tau_\infty}{\rho} = \frac{f_w U_m^2}{2} \tag{2.5}$$

where U_m is the undisturbed linear near-bed orbital velocity amplitude and f_w is the friction factor, given from Myrhaug et al. (2001)

$$f_w = c(\frac{A}{z_0})^{-d} \tag{2.6}$$

$$(c,d) = (18,1) \quad for \quad 20 \lesssim A/z_0 < 200$$

$$(c,d) = (1.39,0.52) \quad for \quad 200 \leqslant A/z_0 < 11000$$

$$(c,d) = (0.112,0.25) \quad for \quad 11000 \leqslant A/z_0$$

where z_0 is the bed roughness and determined by $z_0 = d_{50}/12$ (Soulsby(1997)). $A = U/\omega$ is the near-bed orbital displacement amplitude and $\omega = 2\pi/T$ is the angular wave frequency where T is the wave period..

Myrhaug et al. (2001) stated that this molding for estimating bottom shear stress is valid in combined waves plus current for wave-dominated flow. By utilizing this friction factor it is possible to find an analytic solution in both waves alone case and waves plus current case.

Chapter 3

Mechanisms of Scour Around Marine Structures

3.1 Scour around a vertical pile

Vertical piles are quite common in marine environment, such as the legs of an offshore platform and the foundation of an offshore wind turbine. When a vertical pile is installed on an erodible seabed, the down-flow in front of the pipe causes a horseshoe vortex that lifts the sediment which is taken away by the flow. At the downstream side of the pipe, a lee-wake vortex is formed due to the flow separation at the side of the pile. Those two vortices are the main reason for scour around a vertical pile.

The horseshoe vortex will be formed if there is rotation in the coming flow. When a vertical pile is installed on the seabed, the boundary layer approaching the pile experiences an adverse pressure gradients in the direction of mainstream. Consequently, the boundary layer on the bed upstream of the pile undergoes a three-dimensional separation (along the dashed line, S, in Fig. 3.1). The separated boundary layer rolls up downstream of the separation line to form a system of horseshoe vortices around the pile. Fig. 3.1 is a definition sketch of vortices around a pile in a flow.

For a pile exposed to a steady current, the horseshoe vortex is influenced by the ratio of the bed boundary layer thickness to the pile diameter, δ/D; the pile Reynolds number, $R_{e_D} = UD/\nu$, where U is the velocity at the outer edge of the bed boundary layer and ν is the kinematic viscosity of the flow; and the pile geometry. Sumer and Fresød (2002) stated that δ/D and R_{e_D} influence the separation of the bed boundary layer and therefore the horseshoes vortex. The separation of the bed boundary layer will be delayed for small δ/D and subsequently result in a small-size horseshoe vortex, as well as for small R_{e_D}. If the

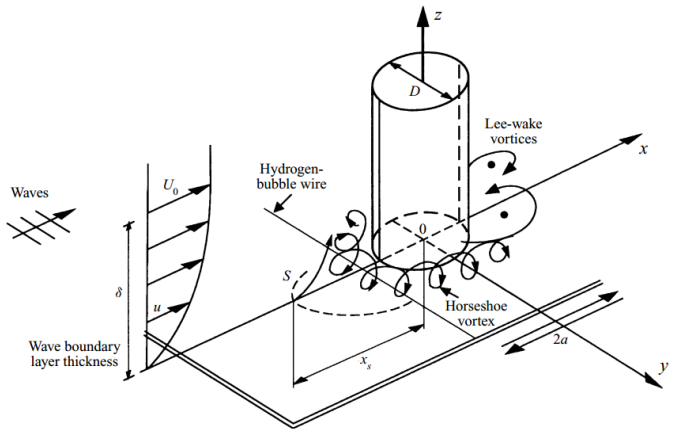

Fig. 3.1 Flow around a vertical pile (from Roulund et al. (2005)).

value of δ/D or R_{e_D} is small enough, the boundary layer may not separate at all, and hence no horseshoe vortex will be formed. Sumer and Fresød (2002) also displayed the bed shear stress underneath a horseshoe vortex in a steady current. Fig. 3.2 shows the mean bed shear stress measured along the principal axis x normalized by the undisturbed mean bed shear stress, $\overline{\tau}/\overline{\tau}_\infty$. It clearly appears that the bed shear stress underneath the horseshoe vortex in front of the pile is larger than the undisturbed bed shear stress.

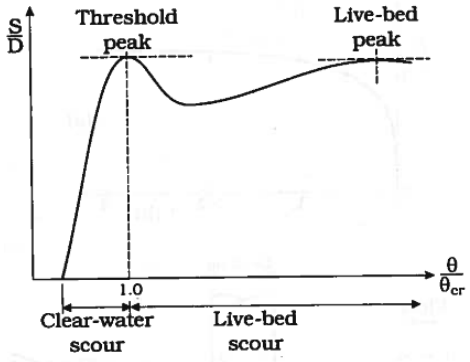

Fig. 3.2 Bed shear stress at the horseshoe vortex side of pile. x=0 coincides with pile axis (from Sumer and Fredsøe (2002)).

For a pile standing in waves, the Keulegan-Capenter number, *KC* is an additional parameter that influences the horseshoe vortex. *KC* number represents the ratio of the orbital displacement of the water particles and the diameter of the pile. For small KC number, the orbital displacement of water particles is small compared with the pile diameter, therefore, the boundary layer may not be separated, then horseshoe vortex may not be formed. For very large *KC* number, the orbital displacement is so large that the flow can be regard as

a steady current for each half period. The horseshoe vortex in such a large KC number is expected to behave similarly as in a steady current.

Sumer et al. (1997) investigated the existence of horseshoe vortex in waves experimentally. Fig. 3.3 displays the horseshoe vortex in phase space. The reason for the asymmetric behavior in the graphs is due to non-linearity of the waves. $\omega t = 0$ corresponds to the zero up-crossing in the orbital velocity near the seabed and apparently there is no horseshoe vortex formed for any KC number in this phase. Their data reveals that the three-dimensional separation occur after KC number reaches the value of 6.

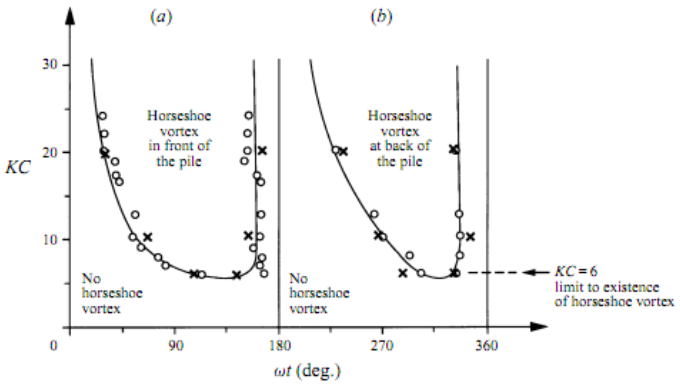

Fig. 3.3 The horseshoe vortex in phase space (from Sumer and Fredsøe (2002)).

The lee-side vortices, on the other hand, are caused by the rotation in the boundary layer over the surface of the pile: the shear layers emanating from the side edges of the pile roll up to form these vortices (see Fig. 3.1).

For a pile installing in a steady current, lee-wake flow is described mainly by the pile Reynolds number, R_{e_D} and pile geometry. In the case of waves, Williamson (1995) studied the vortex flow behind a free cylinder subjected to an oscillatory flow. Sumer and Fredsøe (1997) investigated those vortex-flow behind a vertical cylinder fixed in the seabed. Their studies demonstrated that the near-bed lee-wake flow has a wide range of vortex-flow regimes, depending on KC number.

3.2 Scour below a pipeline

Marine pipelines are installed in seabed to mainly transport gas and crude oil from the offshore platform in oil and gas industry. When a pipeline placed on erodible seabed is exposed to flow, scour may be initiated as the result of piping mechanism. The development

of scour can usually be divided into four stages: onset of scour, tunnel erosion, lee-wake erosion and the final equilibrium stage.

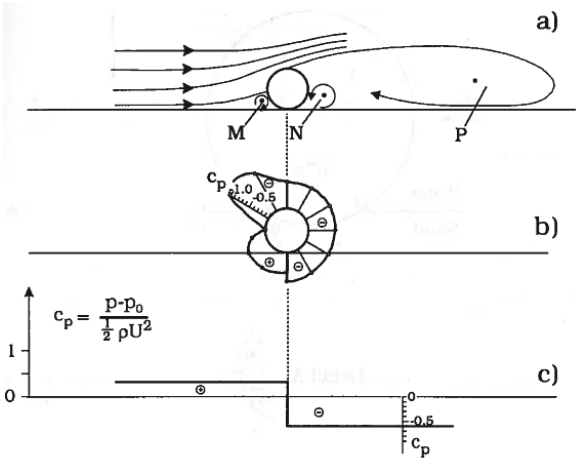

Fig. 3.4 Pressure distributions for bottom-seated pipe (from Sumer and Fredsøe (2002)).

The onset of scour is related to a seepage flow. A pipeline placed on a sandy seabed in a transverse current experiences a pressure difference between the upstream and the downstream sides of the pipeline (See Fig. 3.4). The pressure difference will induce a seepage flow underneath the pipe. For a sufficiently large current velocity, the surface of the sand will rise at the downstream of the pipe and then a mixture of sand and water will break through the space underneath the pipe. This process is called piping, which starts the onset of scour. Fig. 3.5 shows the procedure of piping. In the case of waves, the variation of wave height affects the breakthrough process. Sumer and Fredsøe also investigated the onset of scour in waves. They found that the onset of scour takes place only in the crest-half, while the pressure gradient in trough-half period is not large enough to onset of scour.

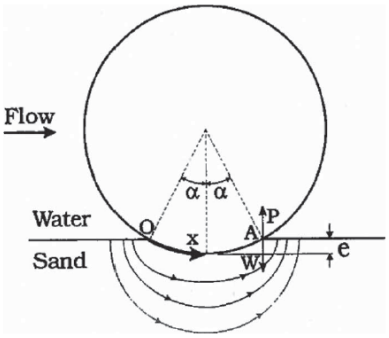

Fig. 3.5 Seepage flow underneath the pipe (from Sumer and Fredsøe (2002)).

The next stage is followed by the tunnel erosion. In this stage, the onset of scour and pipe has started. There is a small gap, e, between seabed and pipe i.e. $e \ll D$ (See Fig. 3.6). But a substantial amount of water will be diverted through the small gap, leading to very large flow velocity in the gap. This results in very large shear stresses on the bed just below the pipeline. This means a tremendous increase in sediment transport capacity. At the end of this stage, the flow velocity will decrease as the gap becomes larger.

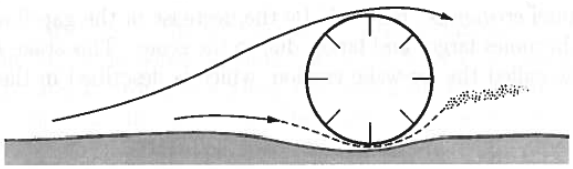

Fig. 3.6 Tunnel erosion below a pipeline (from Sumer and Fredsøe (2002)).

When the gap between seabed and pipeline reaches a critical value, vortex-shedding will occur behind the pipeline. The scour will be subsequently governed by the vortex shedding. This stage is called the lee-wake erosion (see Fig. 3.7). In this stage, the sediment transport capacity increases significantly due to rapid increase of bed shear stress.

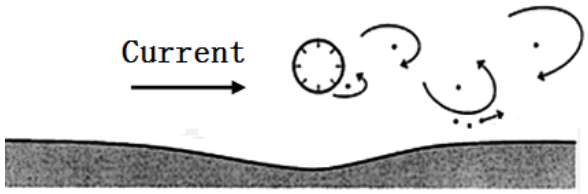

Fig. 3.7 Lee-wake below a pipeline in current (from Sumer and Fredsøe (2002)).

Finally, the scour process reaches a steady state that is called equilibrium stage. In this stage the bed shear stress along the bed underneath the pipe equals to its undisturbed value. That means the amount of sediments that enters the scour hole is identical to that leaving the scour hole.

When pipelines is exposed to waves, it experiences piping from both side. Sumer and Fredsød (2002) stated that the main difference between waves case and a steady current case is that the downstream wake system now occurs on both sides of the pipeline (See Fig. 3.8)

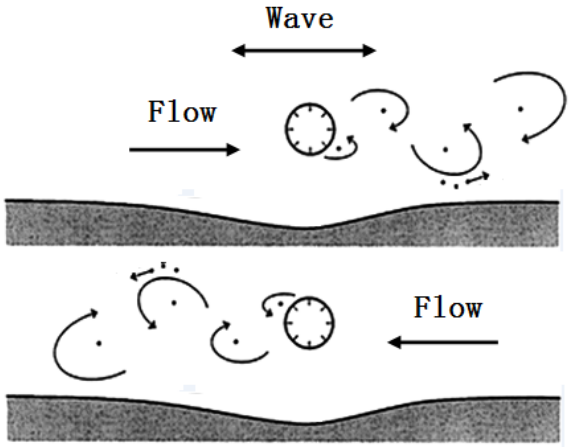

Fig. 3.8 Lee-wake below a pipeline in waves (from Sumer and Fredsøe (2002)).

Chapter 4

Background for Scour in Regular Waves

4.1 Scour around a vertical pile

Sumer et al. (1992b) investigated the scour around a single, slender vertical pile with a circular cross-section in regular waves through laboratory tests. They obtained the following empirical formula for the equilibrium scour depth S with diameter D (see Fig. 4.1) for live-bed condition,

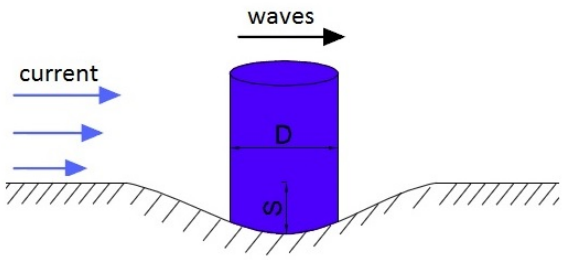

Fig. 4.1 Definition sketch of scour depth S around a vertical pile with diameter D.

$$\frac{S}{D} = C\{1 - \exp[-q(KC - r)]\}; \quad for \quad KC \geqslant r \tag{4.1}$$

where C, q and r are coefficients given by the following values

$$(C,\ q,\ r) = (1.3,\ 0.03,\ 6) \tag{4.2}$$

where the Keulegan-Carpenter number, KC is defined as

$$KC = \frac{UT}{D} \tag{4.3}$$

It should be noted that for the steady current case ($T \to \infty$ and thus $KC \to \infty$), S/D will approach to $C = 1.3$. The Eqs. (4.1) and (4.2) are valid when the storm has lasted longer than the time scale of the scour. Further details on the time scale of the scour are given in Sumer et al. (1992a).

Alternatively, KC can be determined by

$$KC = \frac{2\pi A}{D} \tag{4.4}$$

Based on the linear wave assumption, the near-bed wave induced displacement amplitude A and velocity U are related to the linear wave height H by

$$A = \frac{H}{2\sinh kh} \tag{4.5}$$

and

$$U = \omega A = \frac{\omega H}{2\sinh kh} \tag{4.6}$$

moreover, by combining Eqs. (4.5) and (4.6) it follows that

$$\omega = \frac{U}{A} \tag{4.7}$$

where k is the wave number, determined from the dispersion relationship

$$\omega^2 = gk\tanh kh \tag{4.8}$$

where h is the water depth, g is the gravity acceleration.

4.2 Scour below marine pipeline

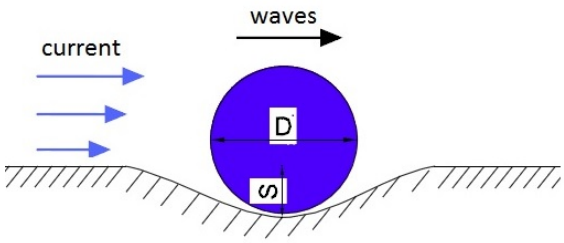

Fig. 4.2 Definition sketch of scour depth S below a pipeline with diameter D.

Sumer and Fredsøe (1990) carried out experiments to study the scour below a fixed

pipeline exposed to regular waves for flat seabeds. They proposed the following empirical formula for the equilibrium scour depth S below the pipeline with diameter D (see Fig. 4.2) for live-bed condition,

$$\frac{S}{D} = 0.1KC^{0.5} \quad for \quad 2 \leq KC \leq 1000 \tag{4.9}$$

Chapter 5

Stochastic Method and Wave Height Distribution

5.1 Introduction

In this chapter, a tentative stochastic method will be outlined. By means of this method, the scour depth around the marine structures subjected to random waves plus current for mild slopes can be derived. Moreover, Battjes and Groenendijk (2000) wave height distribution based on laboratory experiment on shallow foreshore will be introduced as well as the truncated distribution function.

5.2 Stochastic method

The stochastic method proposed here is based on the following assumptions: (1) the storm has lasted long enough to develop the equilibrium scour depth; (2) Only the highest waves are responsible for the scour response. The highest waves considered here are those exceeding the probability $(1/n)th$, denoted by $H_{1/n}$. Here the highest among random waves in a stationary narrow-band sea state are considered. The quantity of interest here is the expected value of maximum equilibrium scour depth caused by the $(1/n)th$ highest waves, which is given as

$$E\left[S(H)|H > H_{1/n}\right] = n\int_{H_{1/n}}^{\infty} S(H)p(H)dH \tag{5.1}$$

where $S(H)$ is the equilibrium scour depth that will be given in the following chapters and $p(H)$ is the probability density function (pdf) of H.

Based on the present assumption, the free surface elevation $\zeta(t)$ is a stationary Gaussian

narrow-band random process with zero expectation described by the single-sided spectral density $S_{\zeta\zeta}(\omega)$. Based on that, the time-dependent near-bed orbital displacement $a(t)$ and velocity $u(t)$ in deep water are both stationary narrow-band process with zero expectation described by spectral densities

$$S_{aa}(\omega) = \frac{S_{\zeta\zeta}(\omega)}{\sinh^2 kh} \tag{5.2}$$

$$S_{uu}(\omega) = \omega^2 S_{aa}(\omega) = \frac{\omega^2 S_{\zeta\zeta}(\omega)}{\sinh^2 kh} \tag{5.3}$$

5.3 Wave height distribution

5.3.1 Battjes and Groenendijk distribution

This thesis focuses on the scour around marine structures on a sloping seabeds in finite water depth. In such condition, the water depth is limited and wave breaking process is involved. Thus the wave height distribution is no longer Rayleigh distribution as it is for non-breaking waves in deep water. Here the Battjes and Groenendijk (2000) wave height distribution based on laboratory experiments on shallow foreshores is employed. The cumulative distribution function (cdf) consists of two two-parameter Weibull distribution, given by

$$F_{\hat{H}} \equiv P(\hat{H} \leqslant \hat{H}) = \begin{cases} P_1(\hat{H}) = 1 - \exp\left[-\left(\frac{\hat{H}}{\hat{H}_1}\right)^{k_1}\right], & \hat{H} \leq \hat{H}_{tr} \\ \\ P_2(\hat{H}) = 1 - \exp\left[-\left(\frac{\hat{H}}{\hat{H}_2}\right)^{k_2}\right], & \hat{H} \geq \hat{H}_{tr} \end{cases} \tag{5.4}$$

It should be noted that we normalize all wave heights with H_{rms}, to be indicated as

$$\hat{H}_x = \frac{H_x}{H_{rms}} \tag{5.5}$$

where, exponent $k_1 = 2$ and $k_2 = 3.6$. H_{tr} is the transitional wave height, given by

$$H_{tr} = (0.35 + 5.8 \tan\alpha)h \tag{5.6}$$

α is the slope angle. *Rms* value of wave height H_{rms} is given as

$$H_{rms} = (2.69 + 3.24\sqrt{m_0}/h)\sqrt{m_0} \tag{5.7}$$

where m_0 is the zeroth spectrum moment.

5.3.2 Prediction of parameters

Battjes and Groenendijk (2000) wave height distribution is a point model which can be calculated for a given water depth h, a slope angle α as well as the zeroth spectrum moment m_0. For a given seabed condition, the water depth can be determined from simple geometric computation. For m_0, it can be obtained from

$$m_0 = \int_0^\infty S_{\zeta\zeta}(\omega,\, h)d\omega \tag{5.8}$$

where $S_{\zeta\zeta}(\omega,\, h)$ is the wave spectrum in finite water depth. According to Young (1999) and Jensen (2002), $S(\omega,\, h)$ can be obtained by multiplying the wave spectrum in deep water $S_{\zeta\zeta}(\omega)$ with a depth correction factor $\varphi(\omega,\, h)$ as

$$S_{\zeta\zeta}(\omega,\, h) = \varphi(\omega,\, h)S_{\zeta\zeta}(\omega) \tag{5.9}$$

where,

$$\varphi(\omega,h) = \frac{\omega^6}{(gk)^3\left[\tanh kh + kh\left(1-\tanh^2 kh\right)\right]} \tag{5.10}$$

For a given h, α and m_0, the values of $\hat{H}_1$ and $\hat{H}_2$ can be either read from Table 2 in Battjes and Groenendijk (2000), or they can be determined by solving the following two equations together:

1) The distribution function has to be continuous, given by

$$F_1(\hat{H}_{tr}) = F_2(\hat{H}_{tr}) \tag{5.11}$$

2) The mean square normalized wave height, or the second moment of the pdf of the truncated CWD of $\hat{H}$, has to equal to unity, given by

$$\int_0^{\hat{H}_{tr}} \hat{H}^2 p_1(\hat{H})d\hat{H} + \int_{\hat{H}_{tr}}^\infty \hat{H}^2 p_2(\hat{H})d\hat{H} = 1 \tag{5.12}$$

where p_1 and p_2 are the probability density function of $\hat{H}$ and defined as: $p_1 = dP_1$, $p_2 = dP_2$. The expression of p_1 and p_2 are given in in Appendix A.

5.3.3 Truncated distribiton

If $\hat{H}$ is defined within a limited inter value $\hat{H} \geqslant \hat{H}_t$, then $\hat{H}$ follows the truncated distribution given by

$$F_{\hat{H}} \equiv P(\hat{H} \leqslant \hat{H}) = \begin{cases} P_1(\hat{H}) = 1 - \exp\left[-\left(\frac{\hat{H}}{\hat{H}_1}\right)^{k_1} + \left(\frac{\hat{H}_t}{\hat{H}_1}\right)^{k_1} \right], & \hat{H}_t \leq \hat{H} \leq \hat{H}_{tr} \\ \\ P_2(\hat{H}) = 1 - \exp\left[-\left(\frac{\hat{H}}{\hat{H}_2}\right)^{k_2} + \left(\frac{\hat{H}_t}{\hat{H}_2}\right)^{k_2} \right], & \hat{H} \geq \hat{H}_{tr} \end{cases} \tag{5.13}$$

For truncated distribution, the only way to determine the values of $\hat{H}_1$ and $\hat{H}_2$ is to solve the Eqs. (5.11) and (5.12) together. But it should be emphasized that the lower limit of integral for the first term in Eq. (5.12) should be $\hat{H}_t$.

Chapter 6

Scour Around a Vertical Pile in Random Waves Plus Current

6.1 Introduction

The stochastic approach, presented in the previous chapter, will be used here to evaluate the scour depth on mild sloping seabeds. The focus of this chapter is on the scour depth around a vertical pile exposed to random waves and combined random waves plus current. This stochastic method is achieved by combining the Sumer and Fredsøe (2001) scour formula for flat seabeds and the Battjes and Groenendijk (2000) wave height distribution for mild slopes. This approach is also based on assuming that the experimental formulas for scour depth around a vertical pile in random waves plus current on flat seabeds are valid for regular waves plus current. It should be noted that this approach is only valid for wave-dominant flow.

6.2 Scour in random waves

6.2.1 Random waves

Sumer and Fredsøe (2001) presented the results of an experimental study on scour around a vertical pile exposed to irregular waves. They found that their empirical formula of the equilibrium scour depth for regular waves given in Eqs. (4.1) and (4.2) can be used for irregular waves provided that KC number is replaced by KC_{rms}, given by

$$KC_{rms} = \frac{U_{rms}T_p}{D} = \frac{2\pi A_{rms}}{D} \tag{6.1}$$

For a fixed location with water depth h, *Rms* value of near-bed wave induced displacement A_{rms} and velocity U_{rms} can be obtained by (based on the linear wave assumption)

$$A_{rms} = \frac{H_{rms}}{2\sinh kh} \tag{6.2}$$

$$U_{rms} = \omega_p A_{rms} = \frac{\omega_p H_{rms}}{2\sinh kh} \tag{6.3}$$

moreover, by combining Eqs. (6.2) and (6.3) it follows that

$$\omega_p = \frac{U_{rms}}{A_{rms}} \tag{6.4}$$

where $\omega_p = 2\pi/T_p$ is the spectral peak frequency, T_p is the spectral peak period, and k_p is the wave number corresponding to ω_p, determined from the dispersion relationship

$$\omega_p^2 = g k_p \tanh k_p h \tag{6.5}$$

6.2.2 Random waves plus current

For this case, Sumer and Fredsøe (2001) found that their empirical formulas for the equilibrium scour depth for regular waves given in Eqs. (4.1) and (4.2) can be also used for combined waves plus current provided that the coefficients q and r are determined by

$$q = 0.03 + 0.75 U_{cwrms}^2 \tag{6.6}$$

$$r = 6\exp(-4.7 U_{cwrms}) \tag{6.7}$$

where,

$$U_{cwrms} = \frac{U_c}{U_c + U_{rms}} \tag{6.8}$$

and U_c is the current velocity.

We note that for $U_c = 0$ in Eq. (6.8), Eqs. (6.6) and (6.7) reduce to the wave alone case with coefficient $q = 0.03$ and $r = 6$.

It should be noted that for $0 \leq U_{cwrms} \leq 0.4$, the combined flow is wave-dominated. For $0.4 \leq U_{cwrms} \leq 1$, it is current-dominated.

6.2.3 Regular waves plus current

The stochastic method proposed here is valid only for the wave-dominated flow. Moreover, it is based on assuming that Eqs. (4.1), (6.6) and (6.7) for irregular waves plus current are valid for regular waves plus current provided that U_{cwrms} is replaced by U_{cw}. That means for $0 \leq U_{cwrms} \leq 0.4$,

$$\hat{S} \equiv \frac{S}{D} = C\{1 - \exp[-q(KC - r)]\}; \quad for \quad KC \geqslant r \tag{6.9}$$

where,

$$q = 0.03 + 0.75U_{cw}^2 \tag{6.10}$$

$$r = 6\exp(-4.7U_{cw}) \tag{6.11}$$

where U_{cw} is defined as

$$U_{cw} = \frac{U_c}{U_c + U} \tag{6.12}$$

Based on narrow-band assumption, $\omega = \omega_p$ ($T = T_p$) and $k = k_p$. Then by combining Eq. (4.7) and (6.4) it follows that

$$\hat{U} = \frac{U}{U_{rms}} = \frac{A}{A_{rms}} = \frac{H}{H_{rms}} = \hat{H} \tag{6.13}$$

consequently, KC and U_{cw} can be re-arranged as

$$KC(\hat{H}) = \frac{UT}{D} = \frac{U_{rms}T_p}{D}\hat{U} = \frac{U_{rms}T_p}{D}\hat{H} = KC_{rms}\hat{H} \tag{6.14}$$

$$\hat{U}_{cw}(\hat{H}) = \frac{U_c/U_{rms}}{U_c/U_{rms} + \hat{U}} = \frac{U_c/U_{rms}}{U_c/U_{rms} + \hat{H}} \tag{6.15}$$

It should be noted that Eq. (6.14) is identical to Eq. (4.3), and Eq. (6.15) is identical to Eq. (6.12).

By substituting Eqs. (6.14) and (6.15) into Eq. (6.9)-(6.11) it follows that

$$\hat{S} \equiv \frac{S}{D} = C\{1 - \exp[-q(KC_{rms}\hat{H} - r(\hat{H}))]\}; \quad for \quad H \geq H_t = \frac{r(\hat{H})}{KC_{rms}} \tag{6.16}$$

where

$$q(\hat{H}) = 0.03 + 0.75U_{cw}(\hat{H})^2 \tag{6.17}$$

$$r(\hat{H}) = 6\exp(-4.7U_{cw}(\hat{H})) \tag{6.18}$$

It should be noted that for given values of ω, U_c and h, the wave number k should be determined from the dispersion relationship for regular waves plus current with an angle ϕ to the direction of the wave propagation, which is $\omega = kU_c cos\phi + (gk\tanh kh)^{1/2}$ (Soulsby (1997)). However, the k is not influenced very much by the presence of the current for wave-dominated flow. Therefore, the wave number k can be obtained from the dispersion relationship for waves alone in Eq. (6.5).

Now the mean scour depth around a vertical pile caused by $(1/n)th$ highest waves follows from Eq. (5.1) as

$$E\left[S(\hat{H})|\hat{H} > \hat{H}_{1/n}\right] = n\int_0^\infty S(\hat{H})p(\hat{H})H(\hat{H} - \hat{H}_{1/n})d\hat{H} \tag{6.19}$$

where $\hat{S}(\hat{H})$ is the scour depth around a vertical pile in regular waves plus current, given in Eqs. (6.16)-(6.18). $p(\hat{H})$ is the truncated probability density function (pdf) and determined from Eq. (5.13), i.e. $p_1 = dP_1$ for $\hat{H}_t \leq \hat{H} \leq \hat{H}_{tr}$, $p_2 = dP_2$ for $\hat{H} > \hat{H}_{tr}$ (the expression of the truncated pdf is given in Appendix A); $H(\hat{H} - \hat{H}_{1/n})$ is the Heaviside function, defined as one for $\hat{H} > \hat{H}_{1/n}$ and zero elsewhere; $\hat{H}_{1/n}$ is calculated by solving the equation $1 - P(\hat{H}_{1/n}) = 1/n$.

6.3 Results and discussion

In this section, the results of the Battjes and Groenendijk (2000) wave height distribution on shallow foreshore including breaking process are presented to describe the sea state in finite water depth. A JONSWAP spectrum, which is transformed to the finite water depth, is assumed in deep water. The effect of slopes on scour in random waves is studied. A slope of 1/100 is considered firstly and then other three slopes, 1/50, 1/150 and 1/250, are considered for this purpose. The scour depth around a vertical pile in combined random waves plus current is addressed at the end. The slope of 1/100 and four locations along the sloping seabeds are considered for this purpose.

Fig. 6.1 illustrates the the seabed conditions with slope=1/100: the water depth at the seaward location ($x = 0m$) is $15m$; the horizontal length of sloping seabeds is $600m$; and the diameter of the vertical pile D is $1m$.

From chapter 5 it is known that the wave spectrum in finite water depth $S_{\zeta\zeta}(\omega, h)$ can be obtained from the spectrum in deep water $S_{\zeta\zeta}(\omega)$. Hence, the random waves with a

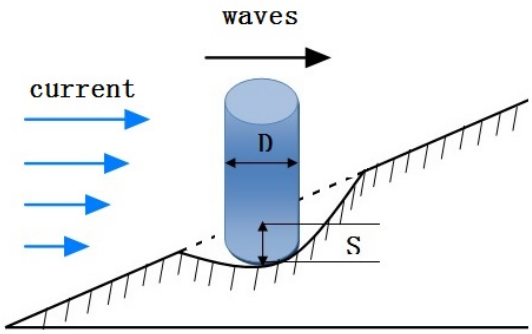

Fig. 6.1 Definition sketch of scour depth S below a vertical pile for mild slopes conditions.

standard JONSWAP spectrum ($\gamma = 3.3$) and significant wave height $H_{m_0} = 8m$ are assumed to describe the sea state in deep water. Fig. 6.2 shows some results of the wave spectra at four locations transformed from the deep water according to Eqs. (5.9) and (5.10). Table 6.1 gives the water depth at each location. In additions, the corresponding values of KC_{rms} and $k_p h$ in each location are presented in Table 6.1. We regard the breaking process as a source of energy dissipation. It is clear in Fig. 6.2 that the wave energy decreases significantly due to the effect of wave breaking. Fig. 6.3 gives the variation of zeroth spectrum moment m_0 with x according to Eq. (5.8). It reveals the fact that breaking activity become more and more pronounced with decreasing of water depths.

Table 6.1 Parameters for the four locations

	Location 1	Location 2	Location 3	Location 4
x (m)	0	200	400	600
$k_p h$	0.77	0.70	0.64	0.57
KC_{rms}	12.73	13.33	13.91	14.57

With the values of m_0 along x, H_{rms} can be determined by Eq. (5.7) and therefore KC_{rms} by Eqs. (6.1) and (6.2). Fig. 6.4 gives the results of KC_{rms} versus x for slope=1/100. It appears that KC_{rms} increases from 13.75 to 15.85 as water depth decreases ($x \longrightarrow 600m$). It needs to be noted that although H_{rms} decreases as x approaches to 600m due to the wave breaking, $k_p h$ decreases because of the limited water depth. Those effects raise the KC_{rms} along x.

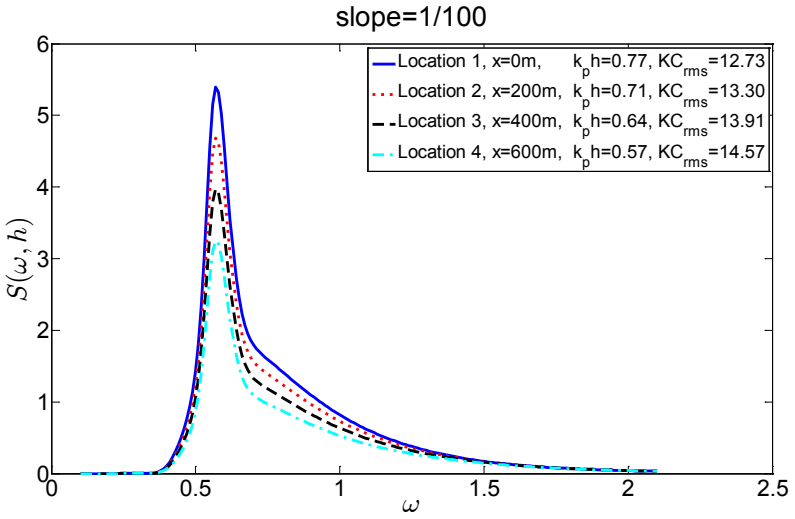

Fig. 6.2 The transitional wave spectra in finite water depth, $S_{\zeta\zeta}(\omega,h)$ (see Eq. (5.9)) versus ω, at four locations for slope=1/100.

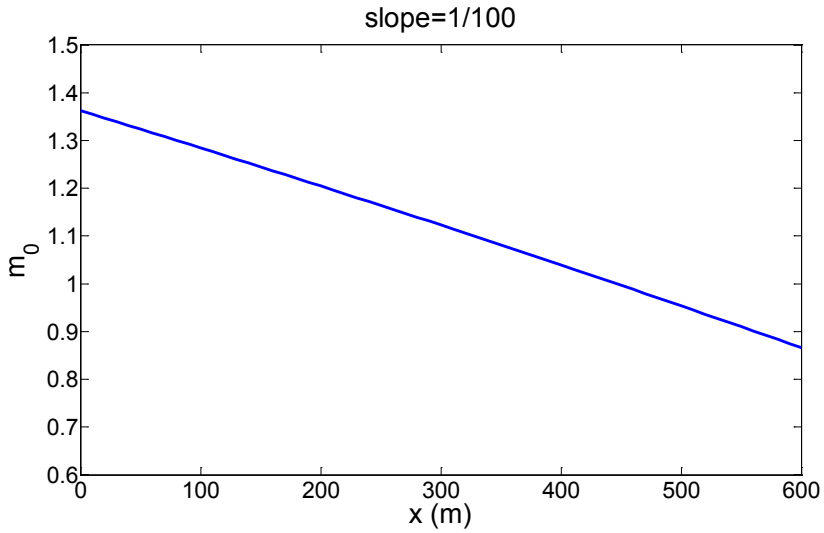

Fig. 6.3 Zeroth spectrum moment, m_0 (see Eq. (5.8)) versus x in finite water depth for slope=1/100.

6.3.1 Waves alone

As mentioned previously in section 3.1, the Sumer and Fredsøe (2002) formulas for scour around a vertical pile (Eqs. (6.16)-(6.18)) are only valid for $\hat{H} \geq \hat{H}_t$ since there is no horseshoe vortex formed for $\hat{H} < \hat{H}_t = r/KC_{rms}$. Hence, the truncated Battjes and Groenendijk (2000) wave height distribution in Eq. (5.13) is required to ensure that all the regular waves considered here have physical meanings. The truncated wave height distribution of

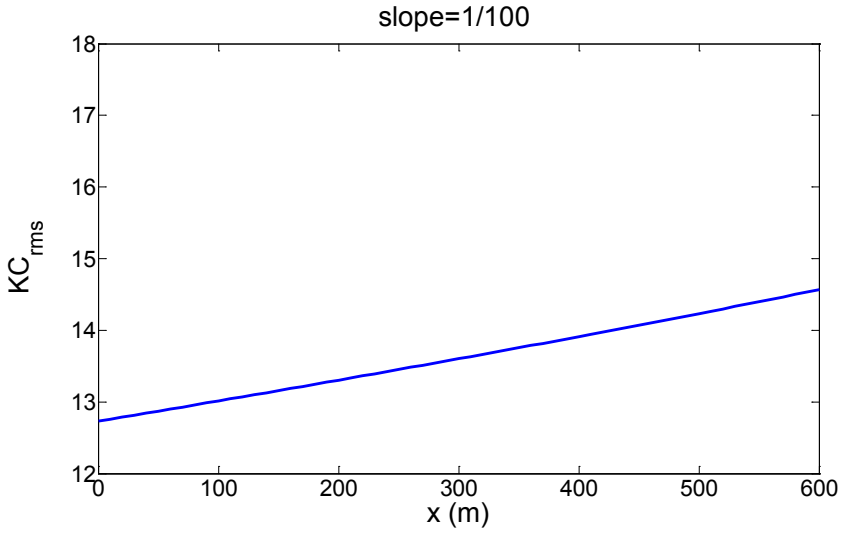

Fig. 6.4 KC_{rms} versus x in finite water depth for slope=1/100.

$\hat{H}$, which is normalized by H_{rms} , are shown in Figs. 6.5 (pdf) and 6.6 (cdf). Four locations (see Table 6.1) are considered here.

The truncation point here, $\hat{H}_t$, indicates the smallest wave height which could be able to form a horseshoe vortex that takes sediment away from the pile. From Fig. 6.5 it appears that $\hat{H}_t$ decreases (slightly) from Location 1 to Location 4, indicating that the threshold of scour decreases as the water depth decreases.

The discontinuous points in Fig. 6.5 are the transitional wave height $\hat{H}_{tr}$, representing the limiting wave height for non-breaking waves. For large $\hat{H}_{tr}$, the distribution reduces to the Rayleigh distribution. The figure shows that from Location 1 to Location 4 (as x increasing from $0 \longrightarrow 600$), $\hat{H}_{tr}$ decreases from 1.78 to 1.30, reflecting that the influence of breaking waves become more and more significant as water depth decreases. It should be noted that the area under each truncated pdf curve must be equal to one, as seen in Fig. 6.6.

Fig. 6.7 illustrates the variation of expected normalized equilibrium scour depth (S/D) around a vertical pipe with the bed length x for slope=1/100. The scour caused by $(1/n)th$ highest waves for n=(3, 10) are denoted by $\hat{S}_{1/3}$ and $\hat{S}_{1/10}$, respectively. It appears that both $\hat{S}_{1/3}$ and $\hat{S}_{1/10}$ increase as water depth decreases (x increases from 0m to 600m). This effect may be attributed to the increase of KC_{rms} alone sloping bed since large KC_{rms} creates more scour. For a given location, $(1/10)th$ highest waves cause more scour than $(1/3)th$ highest waves, i.e. $\hat{S}_{1/10} > \hat{S}_{1/3}$. Further, $\hat{S}_{1/10}$ increases slightly from seaward location at $x = 0$ to the ending point of shore at $x = 600$, while $(1/3)th$ highest waves increase more. The reason is due to the large difference in wave height distribution for $\hat{H} > \hat{H}_{1/3}$ between

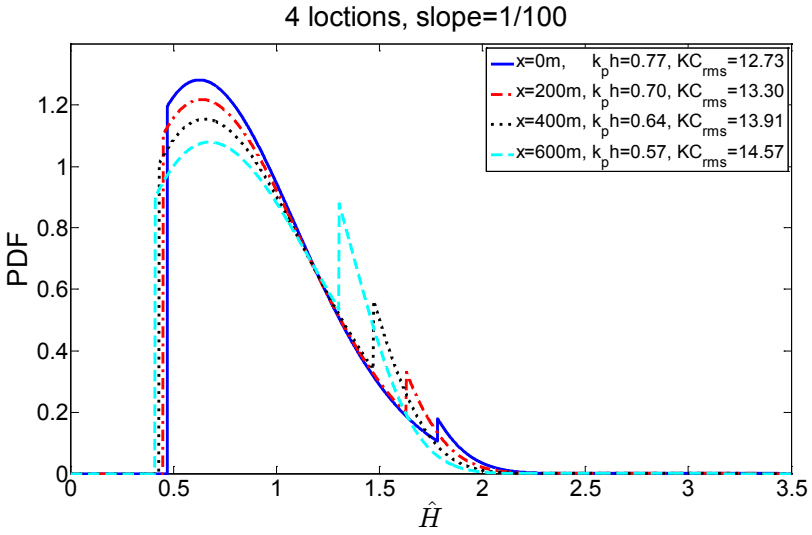

Fig. 6.5 Truncated probability density function of $\hat{H}$ at four locations for slopes=1/100.

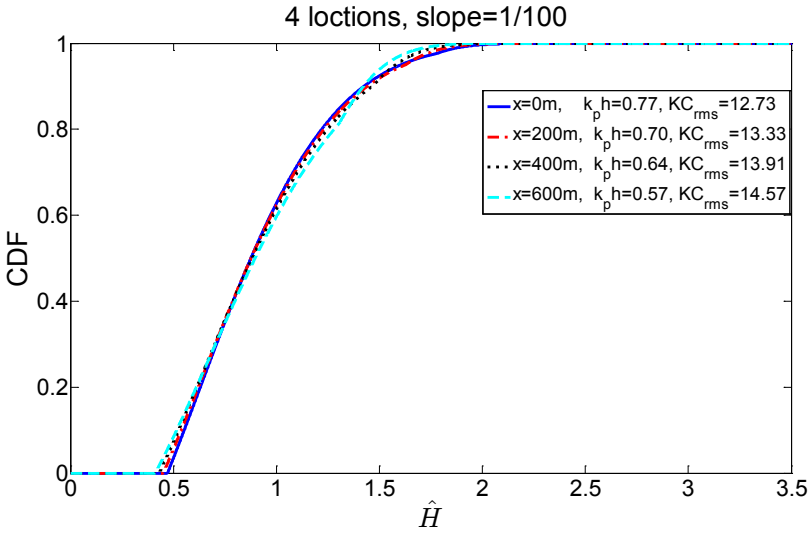

Fig. 6.6 Truncated cumulative distribution function of $\hat{H}$ at four locations for slopes=1/100.

different locations but small difference for $\hat{H} > \hat{H}_{1/10}$. Overall, from the view of scour mechanistic, the results shows that the effect of slope increase the scour depth because the breaking process creates strongly downward direction flow that erodes the seabed.

Now, let us compare the present results with the results from different slopes. Fig. 6.9 shows the KC_{rms} versus x for three additional slopes together with 1/100. The seabed conditions for four slopes can be seen in Fig. 6.8. From Fig. 6.9 it appears that for all slopes, KC_{rms} increases as water depth decreases. KC_{rms} = 12.73 at $x = 0$ for all slopes. Moreover, at a given location x, it appears that KC_{rms} increases as slope increases. It should be

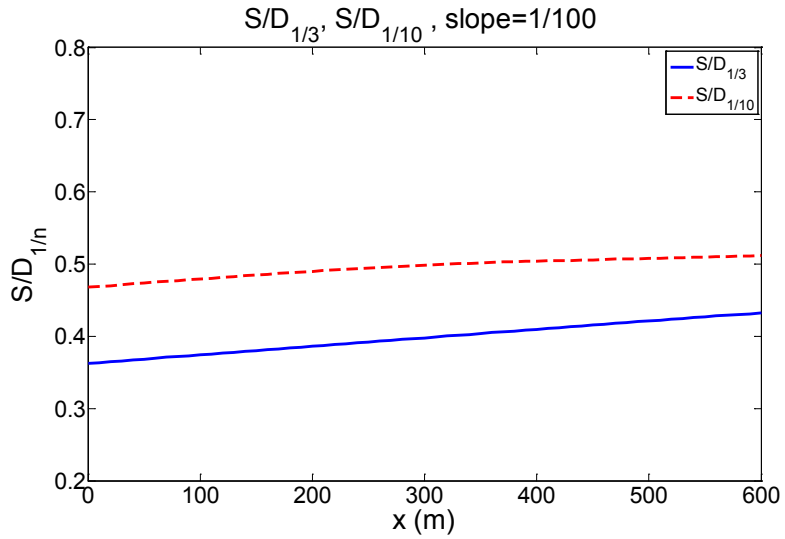

Fig. 6.7 Scour around a pile: maximum scour depth, $\hat{S}_{1/n}$ versus x for n=(3, 10), for waves alone case and slope=1/100.

emphasized that for all slopes, both H_{rms} and $k_p h$ decrease as $x \longrightarrow 600$.

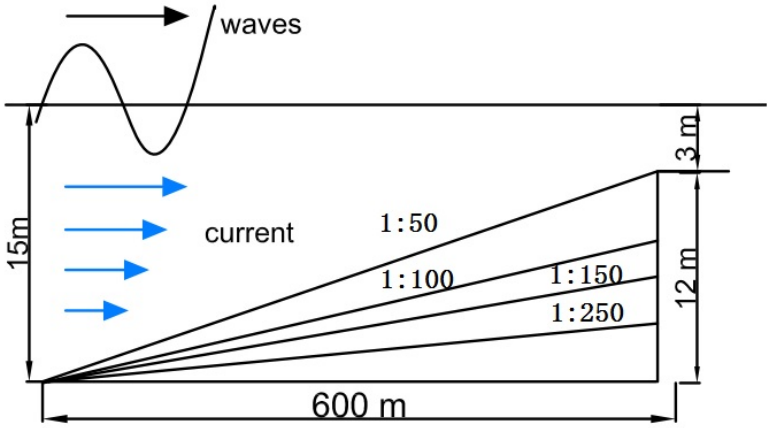

Fig. 6.8 Sketch of seabed conditions for four slopes: 1/50, 1/100, 1/150, 1/250. The total horizontal length of sloping seabed is 600m, the water depth at seaward location is 15m.

Fig. 6.10 shows the equilibrium scour depth around a vertical pile for different slopes. As expected, the effect of slope is to increase more scour. From the figure it is apparent that for all slopes, $\hat{S}_{1/n}$ for $n = (3,\ 10)$ increase as the x approaches to 600m. At a given location x, it shows that $\hat{S}_{1/n}$ increases as slope increases. Those results are completely consistent with those in Fig. 6.9, suggesting that large KC_{rms} causes more scour.

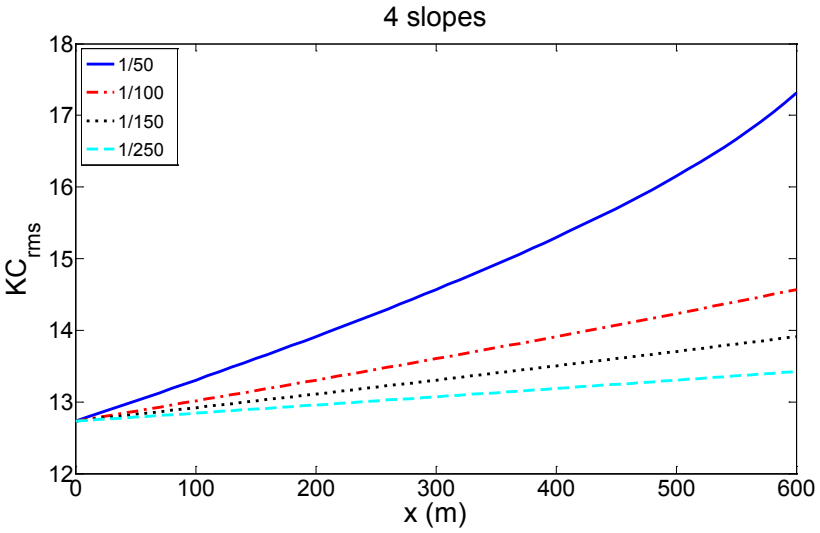

Fig. 6.9 KC_{rms} versus x for four slope: 1/50, 1/100, 1/150, 1/250.

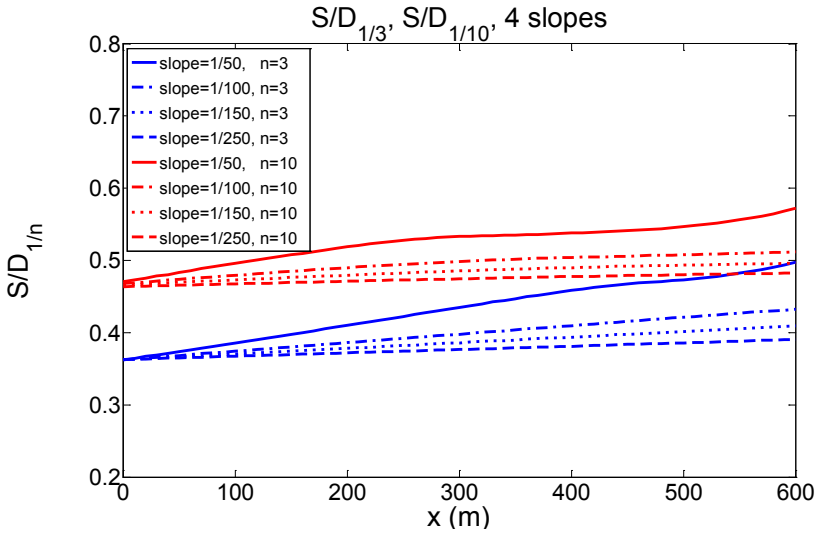

Fig. 6.10 Scour around a pile: maximum scour depth, $\hat{S}_{1/n}$ versus x for n=(3, 10) for waves alone case and four slopes.

6.3.2 Waves plus current

The influence of current on scour depth around a vertical pile will be investigated in this section. This is achieved by changing U_c in U_{cwrms} in Eq. (6.8). Four locations are considered here, as seen in Table 6.1. It should be emphasized that the stochastic method proposed here is valid for wave-dominated flow, i.e. $0 \leq U_{cwrms} \leq 0.4$.

When a current is superimposed on random waves, the truncation point $\hat{H}_t$ which is related to current velocity will be influenced. Consequently, the wave height distribution

of $\hat{H}$ is changed by the present of the current. Fig. 6.11 displays the truncated Battjes and Groenendijk (2000) wave height distribution, with respect to normalized wave height $\hat{H}$, for different values of $U_{cwrms} = U_c/(U_c + U_{rms})$ at Location 1. For other locations, the results are shown in Appendix B.

As Fig. 6.11 suggests, for $U_{cwrms} = 0$, the distribution is consistent with that for wave alone case in Fig. 6.5. As U_{cwrms} increase, the truncation point $\hat{H}_t$ decreases significantly. It is seen that v almost drops to zero when U_{cwrms} up to 0.05. This result implies that, for the weak waves (which are not able to generate scour alone), even a slight current would cause the threshold value of scour $\hat{H}_t$ decreasing significantly. For a given location, the value of transitional wave height is identical because it is independent on the current velocity. Fig. 6.12 gives the results of truncated cumulative distribution in random waves plus current for different values of U_{cwrms}.

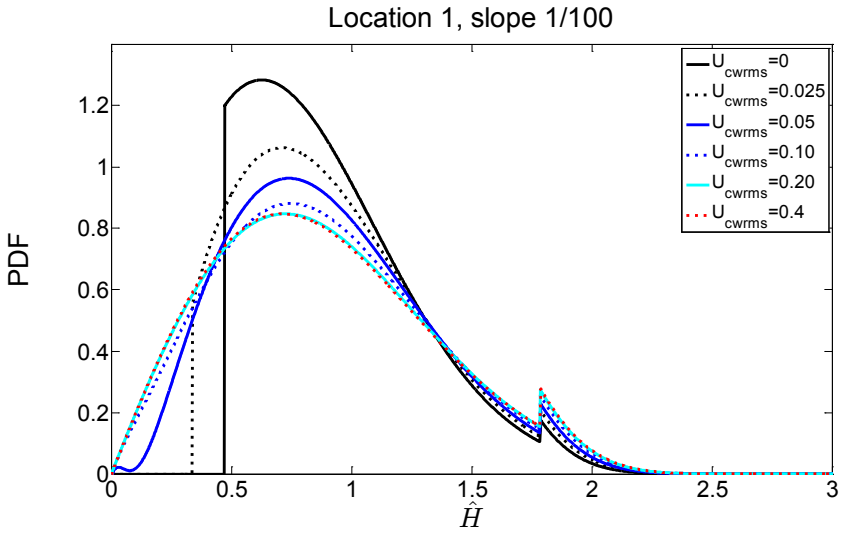

Fig. 6.11 Truncated probability density function of $\hat{H}$ for different U_{cwrms} at four locations. Six values of U_{cwrms} are shows here: $U_{cwrms} = (0,\ 0.0025,\ 0.05,\ 0.1,\ 0.2,\ 0.4)$.

Fig. 6.13 illustrates the expected normalized equilibrium scour depth in combined random waves plus current, with respect to $U_{cwrms} = U_c/(U_c + U_{rms})$ in the range 0-0.4, for slope=1/100 at four locations corresponding to Table 6.1. The expected equilibrium scour depth in combined flow is denoted by $\hat{S}_{cw1/3}$ and $\hat{S}_{cw1/10}$ for n=(3, 10), respectively. The following conclusions can be deduced from Fig. 6.13.

Firstly, It is obvious that $\hat{S}_{cw1/n}$ goes to the results given in Fig. 6.7 as the U_{cwrms} approaches to 0 (waves alone case). The increase of $\hat{S}_{cw1/n}$ from Location 1 to Location 4 at $U_{cwrms} = 0$ implies that the effect of slope increases the scour depth.

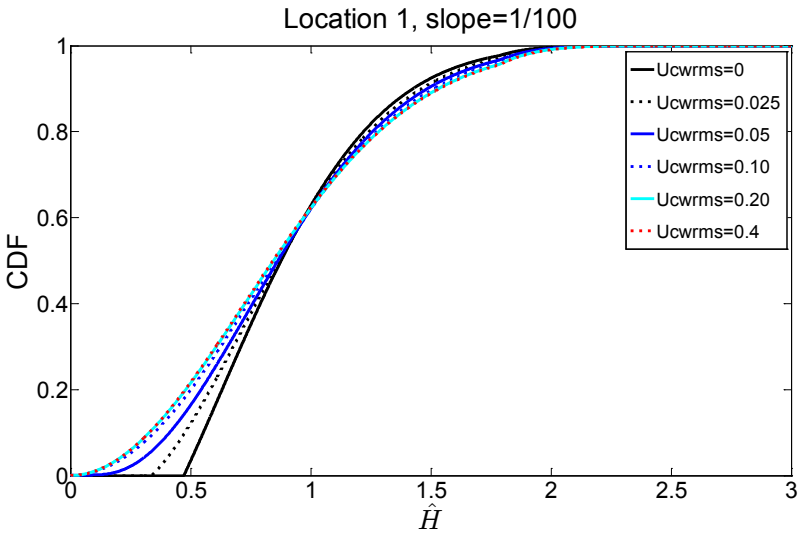

Fig. 6.12 Truncated cumulative distribution function of $\hat{H}$ for different U_{cwrms} at four locations. Six values of U_{cwrms} are shows here: $U_{cwrms} = (0,\ 0.0025,\ 0.05,\ 0.1,\ 0.2,\ 0.4)$.

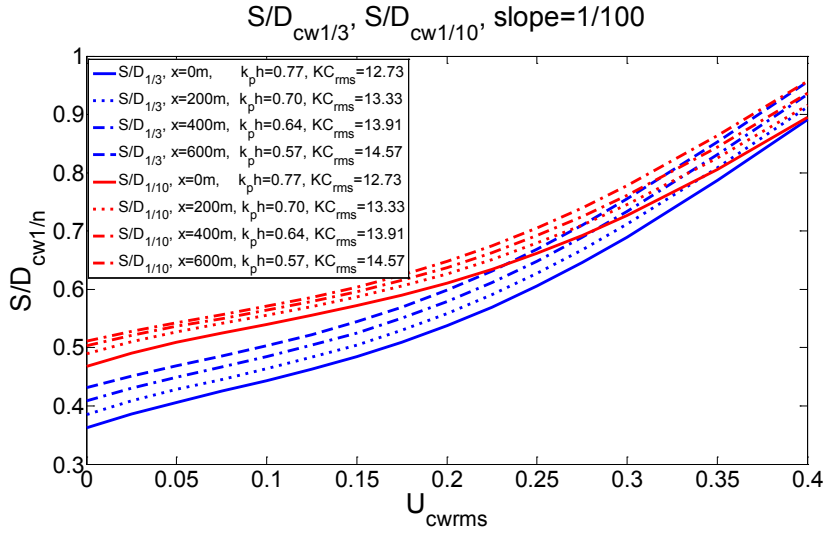

Fig. 6.13 Scour around a pile: maximum scour depth, $\hat{S}_{cw1/n}$ versus U_{cwrms} for n= (3, 10) for waves plus current case and slope= 1/100.

Secondly, it is seen from the Fig. 6.13 that the effect of the current apparently increase the scour depth compared with that for waves alone case. The influence becomes more and more pronounced with increasing U_{cwrms}. More specifically, for all locations, $\hat{S}_{cw1/3}$ and $\hat{S}_{cw1/10}$ at $U_{cwrms} = 0.4$ are around 2.5 times and 1.3 times larger than those for wave alone case, respectively. This is linked to the mechanisms of scour around a vertical piles referred to section 3.2. The strong horseshoe vortex is formed in front of the pile even in the case of a weak current.

Finally, for a given current velocity, the $(1/10)th$ highest waves plus current cause more scour than the $(1/3)th$ highest waves plus current. However, the difference become smaller as U_{cwrms} increases. $\hat{S}_{cw1/3}$ and $\hat{S}_{cw1/10}$ approach to each other as U_{cwrms} approaches to 0.4. The main reason for this is: for small U_{cwrms}, the random waves still is the mainly response for scour depth, but with the increase of U_{cwrms}, the effect of current become pronounced. The flow changes to current-dominant when U_{cwrms} increases to 0.4. In such flow condition, the current becomes the main response for scour depth.

Additionally, similar to waves alone case, for a given location, the equilibrium scour depth caused by $1/10th$ highest is larger than that caused by $1/3th$ highest waves, i.e. $\hat{S}_{cw1/10} > \hat{S}_{cw1/3}$ for the case of waves plus current.

Chapter 7

Scour Below a Pipeline in Random Waves Plus Current

7.1 Introduction

In this chapter, the stochastic method will be used to calculate the scour depth below a pipeline on mild slopes by combining the scour formula for pipelines on flat seabeds and the Battjes and Groenendijk (2000) wave height distribution for mild slopes. Similar to vertical piles, this approach is based on assuming that the experimental formulas for scour depth below a pipeline in random waves plus current on a horizontal bed are valid for regular waves plus current.

7.2 Scour in random waves

7.2.1 Waves alone

Sumer and Fredsøe (1996) presented an experimental study of scour below a pipeline in irregular waves plus current for $5 < KC < 50$ and live-bed conditions. They found that Eq. (4.9) can be used for irregular waves as well provided that the KC number is calculated as KC_{rms} given in Eq. (6.1).

7.2.2 Waves plus current

For combined waves plus current, Sumer and Fredsøe (1996) found the following expression for the scour depth S below a pipeline with diameter D with KC ranging from 5 to about 50.

$$\frac{S}{D} = \frac{S_{cur}}{D} F \tag{7.1}$$

where $S_{cur}/D = 0.6$ is the normalized scour depth for steady-current alone. F is given by the following empirical equations

$$F = \frac{5}{3} KC^a \exp(2.3b) \quad for \quad 0 \leq U_{cwrms} \leq 0.7 \tag{7.2}$$

$$F = 1 \quad for \quad 0.7 \leq U_{cwrms} \leq 1 \tag{7.3}$$

where U_{cwrms} is given by Eq. (6.8), the coefficient a and b are given by

1) For the wave-dominated flow: $0 \leq U_{cwrms} \leq 0.4$

$$a = 0.557 - 0.912(U_{cwrms} - 0.25)^2 \tag{7.4}$$

$$b = -1.14 + 2.24(U_{cwrms} - 0.25)^2 \tag{7.5}$$

2) For the wave-dominated flow: $0.4 \leq U_{cwrms} \leq 1$

$$a = -2.1 U_{cwrms} + 1.46 \tag{7.6}$$

$$b = 3.3 U_{cwrms} - 2.5 \tag{7.7}$$

It is noticed that there is a discontinuity in Eqs. (7.4), (7.5) and Eqs. (7.6), (7.7) at $U_{cwrms} = 0.4$. However, for the wave-dominated flow, this is not an issue since $0 \leq U_{cwrms} \leq 0.4$. Eqs. (7.1), (7.2), (7.4) and (7.5) (wave-dominant flow) will reduce to Eq. (4.9) (wave alone case) if $U_c = 0$ in Eq. (6.8).

Similar to vertical piles case, here only the wave-dominated flow is considered. Moreover, the stochastic method is based on assuming that Eqs. (7.1), (7.2), (7.4) and (7.5) for irregular waves plus current are valid for regular waves plus current provided that U_{cwrms} is replaced by U_{cw}. That means for $0 \leq U_{cwrms} \leq 0.4$,

$$F = \frac{5}{3} KC^a \exp(2.3b) \tag{7.8}$$

and

$$a = 0.557 - 0.912(U_{cw} - 0.25)^2 \tag{7.9}$$

$$b = -1.14 + 2.24(U_{cw} - 0.25)^2 \tag{7.10}$$

By substituting Eqs. (6.14) and (6.15) into Eqs. (7.8)-(7.10), the scour formulas for regular waves plus current is given by

$$\hat{S} \equiv \frac{S}{D} = \frac{S_{cur}}{D} F(\hat{H}) \tag{7.11}$$

where

$$F(\hat{H}) = \frac{5}{3} KC(\hat{H})^a \exp(2.3b) \tag{7.12}$$

and,

$$a(\hat{H}) = 0.557 - 0.912(U_{cw}(\hat{H}) - 0.25)^2 \tag{7.13}$$

$$b(\hat{H}) = -1.14 + 2.24(U_{cw}(\hat{H}) - 0.25)^2 \tag{7.14}$$

Now the mean scour depth below a pipeline caused by $(1/n)th$ highest waves follows from Eq. (5.1) as

$$E\left[S(\hat{H}) | \hat{H} > \hat{H}_{1/n}\right] = n \int_{\hat{H}_{1/n}}^{\infty} \hat{S}(\hat{H}) p(\hat{H}) d\hat{H} \tag{7.15}$$

where $\hat{S}(\hat{H})$ is the equilibrium scour depth below a pipeline, given by Eqs. (7.11)-(7.14); $p(\hat{H})$ is the probability density function (pdf) of $\hat{H}$ and determined from Eq. (5.4), i.e. $p_1 = dP_1$ for $\hat{H} \leq \hat{H}_{tr}$, $p_2 = dP_2$ for $\hat{H} > \hat{H}_{tr}$. The expressions of pdf are found in Appendix A, Eq. (A.3); $\hat{H}_{1/n}$ is calculated by solving the equation $1 - P(\hat{H}_{1/n}) = 1/n$.

7.3 Results and discussion

The seabed conditions used for vertical piles are used here for estimating the scour depth below a pipeline. Fig. 7.1 gives the sketch of scour depth S below a pipeline with a diameter D on the mail sloping seabed.

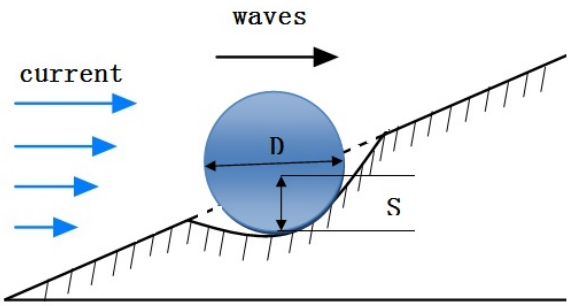

Fig. 7.1 Definition sketch of scour depth S below a vertical pile for mild slopes conditions.

7.3.1 Waves alone

Fig. 7.2 shows the probability density function of $\hat{H}$ at four locations for slope=1/100. It should be noted that for scour below pipelines, no truncation wave height $\hat{H}_t$ exits because there is no restrict condition for threshold of scour. The Battjes and Groenendijk (2000) distribution in Eq. (5.4) is directly used to describe the wave height distribution for mild slopes. It appears that the pdf of $\hat{H}$ almost overlap before wave breaks at $\hat{H}_{tr}$. However, breaking process occurs at different values of $\hat{H}_{tr}$ for different locations. The values of transitional wave heights $\hat{H}_{tr}$ at four locations are exactly identical to that for vertical piles because $\hat{H}_{tr}$ depends on the water depth and slope angle (see Eq. (5.6)). The cumulative distribution function is plotted in Fig. 7.3.

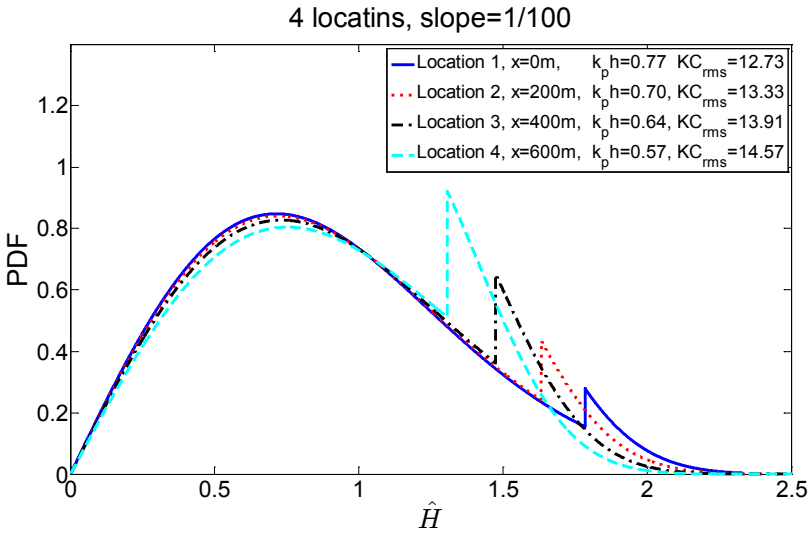

Fig. 7.2 Probability density function of $\hat{H}$ at four locations for slope=1/100.

Fig. 7.4 illustrates the variation of the expected normalized equilibrium scour depth be-

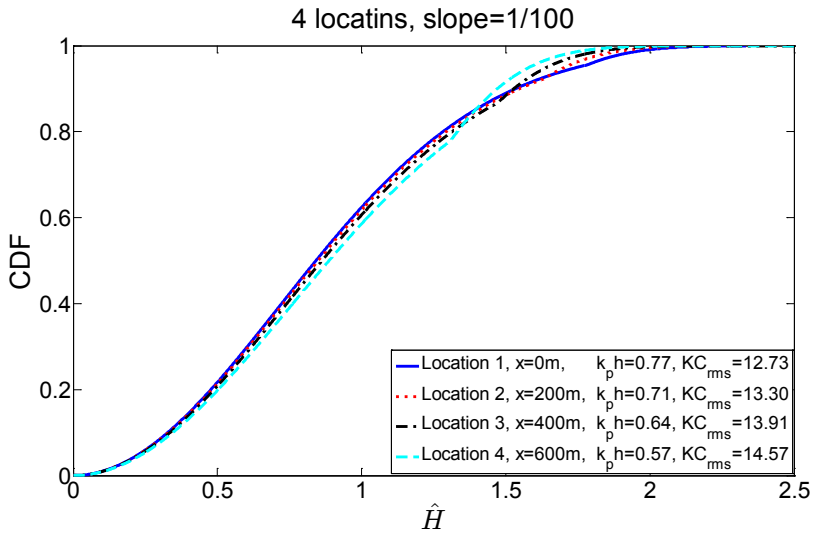

Fig. 7.3 Cumulative distribution function of $\hat{H}$ at four locations for slope=1/100.

low a pipelines with horizontal bed length x for slope=1/100. As defined previously, the scour caused by $(1/n)th$ highest waves for $n = (3,10)$ are denoted by $\hat{S}_{1/3}$ and $\hat{S}_{1/10}$ respectively. Generally, it appears that the $\hat{S}_{1/n}$ increase (slightly) as the water depth decrease ($x \to 600m$). For a given location x the scour depth always appears that $\hat{S}_{1/10} > \hat{S}_{1/3}$. It should be noted that the KC_{rms} is the same as that for the vertical pile case in Fig. 6.4 due to the identical seabeds condition. As explained in section 3.2, for large values of KC_{rms} the lee-wake vortices travel over a larger part of the seabed, and take more sediments away from the pipeline, leading to large scour hole.

Fig. 7.5 shows the comparison of expected normalized equilibrium scour depth $\hat{S}_{1/n}$ below a pipeline at four locations. The corresponding value of KC_{rms} for four sloping seabeds are shown in Fig. 6.9. It can be concluded that for a given location x, large slope causes more scour.

7.3.2 Waves plus current

The effect of current on scour below a pipeline will be studies in this section. Following the same method for vertical piles in section 6.2, the effect of current is considered by changing U_c in U_{cwrms} in Eq. (6.8).

Fig. 7.6 shows the expected normalized equilibrium scour depth below a pipeline exposed to combined waves plus current versus $U_{cwrms} = U_c/(U_c + U_{rms})$ in the range 0-0.4 for slope=1/100 at four locations. The expected equilibrium scour depth in combined flow is denoted by $\hat{S}_{cw1/3}$ and $\hat{S}_{cw1/10}$ for $n = (3,10)$, respectively. It should be noted that the

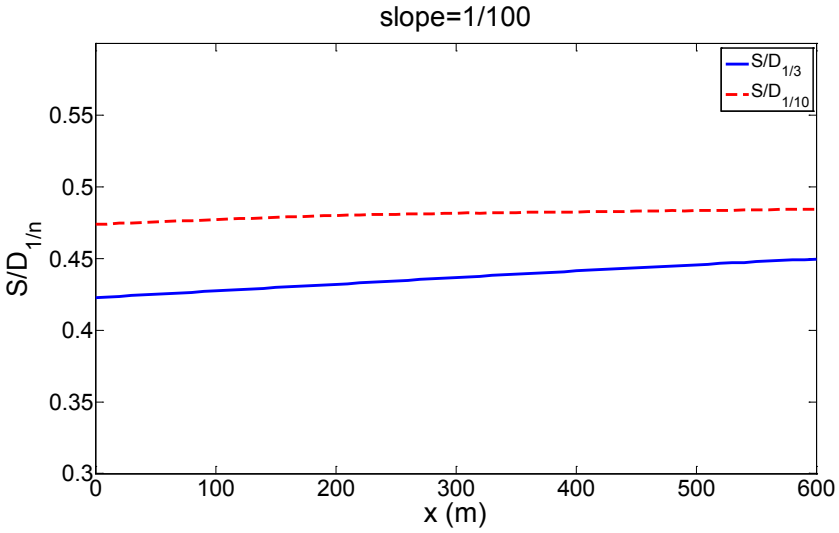

Fig. 7.4 Scour below a pipeline: maximum scour depth, $\hat{S}_{1/n}$ versus x for n=(3, 10) for waves alone case and slope=1/100.

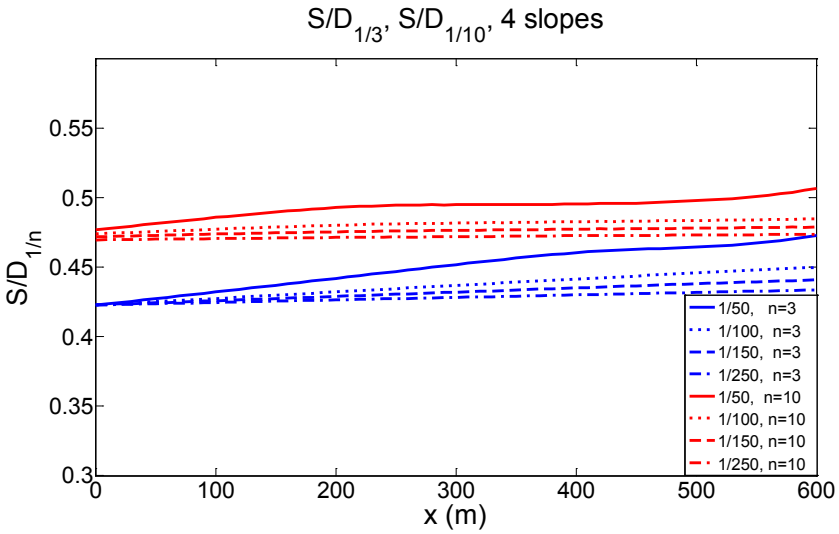

Fig. 7.5 Scour below a pipeline: maximum scour depth, $\hat{S}_{1/n}$ versus x for n=(3, 10) for waves alone case and four slopes.

wave height distribution and KC_{rms} are not influenced by the current. Hence the KC_{rms} in Fig. 6.4, the pdf in Fig. 7.2 and cdf in Fig. 7.3 are still valid for waves plus current case.

Firstly, it is obviously that $U_{cwrms} = 0$ corresponds the wave alone case in Fig. 7.4. The increase of $\hat{S}_{cw1/n}$ from Location 1 to Location 4 at $U_{cwrms} = 0$ implies that the effect of slope increases the scour depth.

Secondly, there is a general trend that, irrespective of locations (KC_{rms} are different at four locations), $\hat{S}_{cw1/n}$ increase as the U_{cwrms} increases from 0 to 0.4, indicating that the

effect of current increases the scour depth compared with that for waves alone. This is linked to the mechanisms of scour below a pipelines referred to section 3.2. Here the current can be considered as a wave with infinite wave period ($KC = +\infty$), resulting in strong ability of sediment transport. Hence, When a current is superimposed on waves, the capacity of sediment transport of the upstream of the scour hole will increase slightly in the direction of flow, leading to increase of scour.

Finally, Fig. 7.6 illustrates that the scour depth $\hat{S}_{cw1/3}$ and $\hat{S}_{cw1/10}$ approach to each other as U_{cwrms} approaches to 0.4. That means the effect of current reduces the difference between the scour caused by different highest waves plus current. This effect is due to: for small U_{cwrms}, the random waves are still mainly response for scour depth, but with the increase of U_{cwrms}, the effect of current becomes pronounced. The flow changes to current-dominant when U_{cwrms} increases to 0.4. In such flow condition, the current becomes the main response for scour depth.

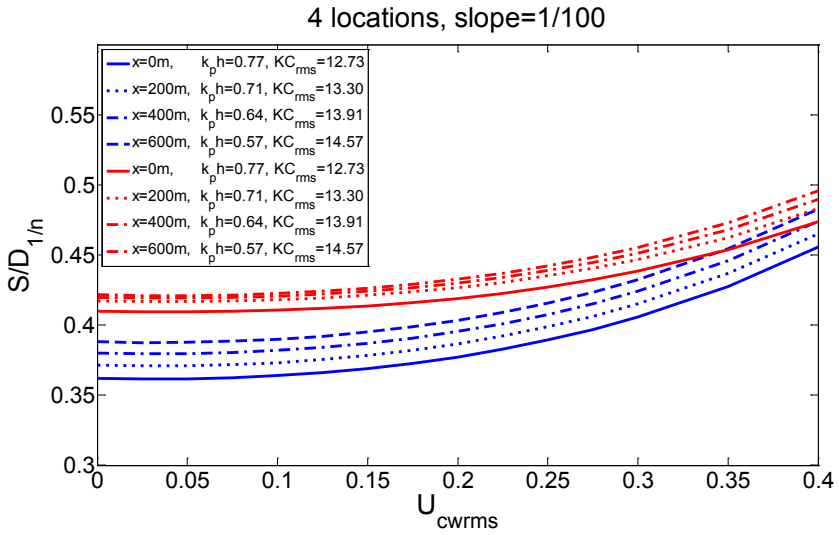

Fig. 7.6 Scour below a pipeline: maximum scour depth, $\hat{S}_{cw1/n}$ versus U_{cwrms} for n= (3, 10) for waves plus current case and slope= 1/100.

Chapter 8

Approximate Method

8.1 Outline of approximate method

Sumer and Fredsøe (1996, 2001) found that the scour formulas for regular waves can be used for random waves if the KC number for regular waves is replaced by KC_{rms} based on H_{rms} and T_p. This is a pragmatic method to evaluate the scour depth around marine structures. Followed by Sumer and Fredsøe's method, an approximated practical method is proposed in this chapter in order to be consistent with the present stochastic method. Then, comparisons are made between the stochastic and approximate method for waves alone case and combined waves plus current case.

Corresponding to the two statistic values of the scour depth $\hat{S}_{1/n}$ for $n = (3, 10)$, it is interesting to know how well the expected equilibrium scour depth caused by $(1/n)th$ highest waves, $E[\hat{S}(\hat{H})|\hat{H} > \hat{H}_{1/n}]$, can be represented by using the mean of the $(1/n)th$ highest wave variable in the scour depth formulas for regular waves, $\hat{S}(E[\hat{H}_{1/n}])$.

For example, alternative KC number for random waves in the approximate method can be defined as

$$KC_{1/n} = \frac{E[U_{1/n}]T_p}{D} = \frac{2\pi E[A_{1/n}]}{D}; \quad for \quad n = (3, 10) \tag{8.1}$$

Based on narrow-band assumption, $E[A_{1/n}]$ and $E[U_{1/n}]$ can be defined as

$$E[A_{1/n}] = \frac{E[H_{1/n}]}{2\sinh k_p h} \tag{8.2}$$

$$E[U_{1/n}] = \omega_p E[A_{1/n}] = \frac{\omega_p E[H_{1/n}]}{2\sinh k_p h} \tag{8.3}$$

where $E[U_{1/n}]$, $E[A_{1/n}]$ and $E[H_{1/n}]$ are the mean values of $(1/n)th$ near-bed orbital displacement amplitude, velocity and wave height, respectively.

8.2 Scour around a vertical pile

The scour depth around a vertical pile for random waves alone can be obtained by replacing KC with $KC_{1/n}$ in Eq. (4.1), given by

$$\frac{S}{D} = C\{1 - \exp[-q(KC_{1/n} - r)]\}; \quad for \quad KC \geqslant r \tag{8.4}$$

$$(C,\ q,\ r) = (1.3,\ 0.03,\ 6)$$

For waves plus current case, it can be obtained by replacing KC with $KC_{1/n}$ in Eqs. (7.1), and U_{cwrms} with $E[U_{1/n}]$ in Eqs. (7.4) and (7.5), given by

$$\hat{S} = C\{1 - \exp[-q(KC_{1/n} - r]\}; \quad for \quad H \geq H_t = \frac{r(\hat{H})}{KC_{1/n}} \tag{8.5}$$

where

$$q = 0.03 + 0.75E[U_{1/n}]^2 \tag{8.6}$$

$$r = 6\exp(-4.7E[U_{1/n}]) \tag{8.7}$$

For scour around a vertical pile exposed to random waves, the results of the stochastic and approximate method ratio for four slopes are shown in Fig. 8.1, denoted by $R_{1/3}$ and $R_{1/10}$ for $n = (3, 10)$, respectively. It interesting to note that the approximate method gives almost the same values as stochastic method for lager slopes, i.e. $1/50$ and $1/100$, while it gives slightly lower values than stochastic one for small slops, i.e. $1/150$ and $1/250$. The difference increases as the water depth decreases. But even for the smallest slope, i.e. $1/250$, the largest ratio is up to around 1.1, which is acceptable in engineering application. Overall, Fig. 8.1 shows that the approximate method can replace the stochastic method for scour around a vertical pile exposed to random waves.

For waves plus current case, Fig. 8.2 gives the result of scour ratio between two methods for slope=1/100. It appears that for all locations, the ratio is lager than one. The difference

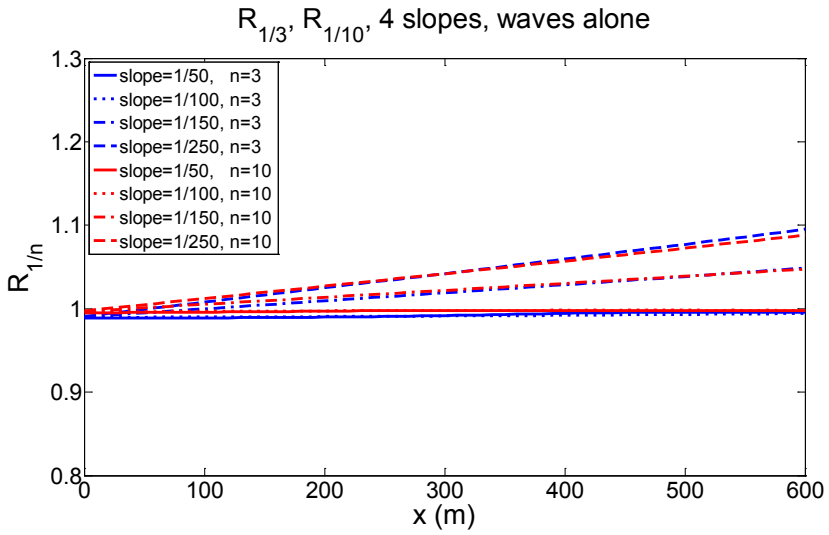

Fig. 8.1 Scour around a pile: stochastic to approximate method ratio, $R_{1/n}$ versus x for n=(3, 10) for waves alone case and four slopes.

between two methods increases as U_{cwrms} increases, suggesting that the effect of current increases the difference between two methods. Overall, the result suggests that the stochastic method can not be replaced by the approximate method for estimating the scour depth around a vertical pile for waves plus current case.

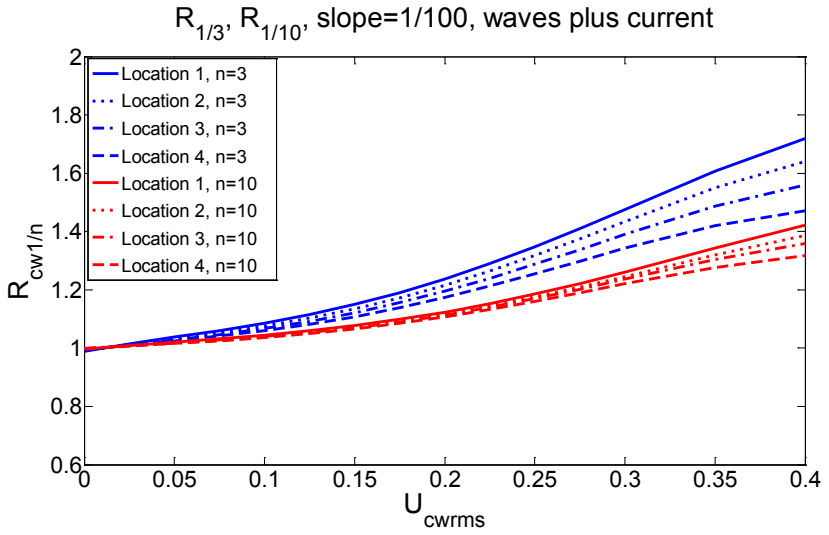

Fig. 8.2 Scour around a pile: stochastic to approximate method ratio, $R_{1/n}$ versus x for n=(3, 10) for waves plus current case and four slopes.

8.3 Scour below a pipeline

The scour depth below a pipeline for waves alone case can be obtained by replacing KC with $KC_{1/n}$ in Eq. (4.9), given as

$$\frac{S}{D} = 0.1KC_{1/n}^{0.5} \tag{8.8}$$

For waves plus current case, it can be obtained by replacing KC and U_{cwrms} with $KC_{1/n}$ and $E[U_{1/n}]$ in Eqs. (7.2), (7.4) and (7.5), respectively, given by

$$\hat{S} = \frac{S_{cur}}{D}\frac{5}{3}KC_{1/n}^{a}\exp(2.3b) \tag{8.9}$$

where

$$a = 0.557 - 0.912(E[U_{1/n}] - 0.25)^2 \tag{8.10}$$

$$b = -1.14 + 2.24(E[U_{1/n}] - 0.25)^2 \tag{8.11}$$

For waves alone, the results of stochastic and approximate method ratio for four slopes are shown in Fig. 8.3, denoted by $R_{1/3}$ and $R_{1/10}$ for $n = (3, 10)$, respectively. It shows that for all slopes, the ratios are very close to 1, especially for n=10, suggesting that the scour depth formula for pipelines exposed to regular waves can be applied for random waves if the random waves are represented by the mean of the $(1/n)th$ highest waves. Thus, to simplify, the approximate method can replace the stochastic method in engineering applications for scour below pipeline in random waves.

For waves plus current, Fig. 8.4 gives the result of scour ratio between the stochastic method and the approximate method for slope=1/100 at four locations, denoted by $R_{cw1/3}$ and $R_{cw1/10}$ for $n = (3, 10)$, respectively. For all locations, it appears that the ratio is about one for U_{cwrms} in the range $0 - 0.15$, while it is lager than one for U_{cwrms} in the range $0.15 - 0.4$. The difference between two methods increases as U_{cwrms} increases, suggesting that the effect of current increases the difference between the stochastic method and the approximate method. Overall, the result shows that the the stochastic method can be replaced by approximate method only for small value of U_{cwrms} for scour below pipeline waves plus current case. It should be noted that those conclusions are based on the condition we discussed in this thesis.

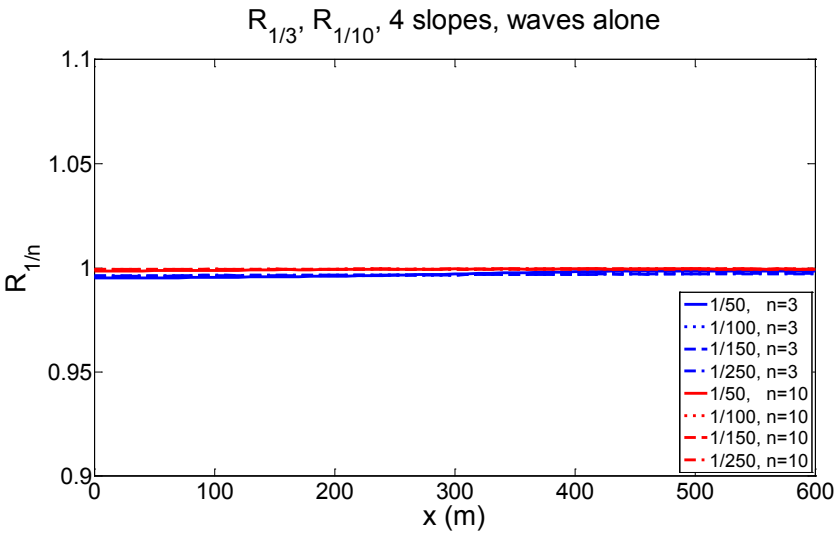

Fig. 8.3 Scour below a pipeline: stochastic to approximate method ratio, $R_{1/n}$ versus x for n=(3, 10) for waves alone case and four slopes.

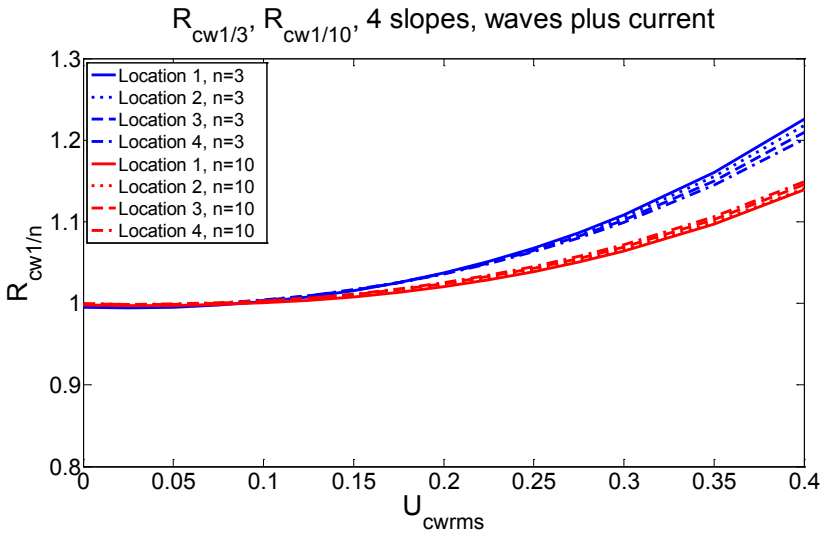

Fig. 8.4 Scour below a pipeline: stochastic to approximate method ratio, $R_{1/n}$ versus x for n=(3, 10) for waves plus current case and four slopes.

Chapter 9

Conclusions

The objective of this thesis is to provide a stochastic method by which the maximum scour depth below marine pipelines and around vertical piles on sloping seabeds for random waves without and with a current can be derived.

The stochastic method introduces a new way to calculate scour depth for mild slope. This is achieved by combining the Sumer and Fredsøe (2002) scour formula for horizontal bed and the Battjes and Groenendijk (2000) wave height distribution for mild slopes.

Scour formulas

Scour depth formulas in regular waves plus current is derived by assuming that Sumer and Fredsøe scour formulas for irregular waves plus current is valid for regular waves plus current provided that U_{cwrms} is replaced by U_{cw}. This is based on the stationary narrow-band assumption.

Wave height distribution

In order to describe the wave condition on sloping seabeds including the breaking process, the Battjes and Groenendijk (2000) wave height distribution for mild slopes is adopted. Battjes and Groenendijk (2000) presented a point model of wave height distribution for a given water depth, a slope angle as well as the zeroth spectrum moment. A method for transformation of spectrum from deep water to finite water depth is presented. The zeroth spectrum moment is calculated by integrating the corresponding wave spectrum. In addition, the truncated wave height distribution is derived for calculating the scour depth around a vertical pile.

Waves alone

Four sloping seabeds are considered to investigate the effect of slope on scour. The present results for the waves alone case reveal that the effect of slope increases scour compared with that at seaward location. The scour depth around a vertical pile and below a

pipeline increase by a factor of about 1.2 and 1.04, respectively, depending on the sloping angle. For both structures, large slopes cause more scour at a fixed location.

Waves plus current

In this case, the mild slope of 1/100 is taken as an example to study the effect of current on scour. The results show that the effect of current increase the scour depth for both structures. This effect become more pronounced as U_{cwrms} increase. The scour depth below pipelines at $U_{cwrms} = 0.4$ is approximately 1.3 times larger than that for the waves alone. For a vertical pile, the scour depth can be 2.5 times larger than that for waves alone..

Approximate method

An approximate method is presented. The ratio between the stochastic method and the approximate method suggests that the approximate method can replace the stochastic method for waves alone case for engineering applications for both pipelines and vertical piles. For waves plus current, however, the approximate method is only applicable for scour below a pipeline for small value of U_{cwrms}. However, for scour around a vertical pipe, the stochastic method should be used.

All the results in this thesis suggest that this stochastic method should be useful as a first approximation in engineering applications when scour depth below marine pipelines and around vertical piles due to random waves plus current is estimated.

Chapter 10

Recommendation for Further Work

The stochastic method proposed in this thesis is based on assuming that the sea state is a stationary narrow-band process. All the results are based on the sea state and seabed conditions exemplified in this thesis. Therefore, more data are required for comparisons in order to give a conclusion regarding the validity of this method. At meantime, experimental study and simulation method should be carried out, providing the data for comparing with present results.

This thesis focuses on scour below marine pipelines and around vertical piles. More other marine structures which may be threatened by scour could be discussed the validity of the stochastic method.

References

Battjes, J. A. and Groenendijk, H. W. (2000). Wave height distributions on shallow foreshores. *Coastal engineering*, 40(3):161–182.

Cevik, E. and Yüksel, Y. (1999). Scour under submarine pipelines in waves in shoaling conditions. *Journal of waterway, port, coastal, and ocean engineering*, 125(1):9–19.

Henry, P.-Y. and Myrhaug, D. (2013). Wave-induced drag force on vegetation under shoaling random waves. *Coastal Engineering*, 78:13–20.

Jensen, J. J. (2002). Conditional short-crested waves in shallow water and with superimposed current. In *ASME 2002 21st International Conference on Offshore Mechanics and Arctic Engineering*, pages 295–300. American Society of Mechanical Engineers.

Kjeldsen, S. P., Gjorsvik, O., Bringaker, K., and Jacobsen, J. (1973). Local scour near offshore pipelines. In *Paper available only as part of the complete Proceedings of the Second International Conference on Port and Ocean Engineering Under Arctic Conditions (POAC), August 27-30, 1973.*

Myrhaug, D., Holmedal, L. E., Simons, R. R., and MacIver, R. D. (2001). Bottom friction in random waves plus current flow. *Coastal engineering*, 43(2):75–92.

Myrhaug, D. and Ong, M. C. (2009). Burial and scour of short cylinders under combined random waves and currents including effects of second order wave asymmetry. *Coastal Engineering*, 56(1):73–81.

Myrhaug, D. and Ong, M. C. (2012). Scour around spherical bodies due to long-crested and short-crested nonlinear random waves. *Ocean System Engineering*, 2(4):257–269.

Myrhaug, D. and Ong, M. C. (2014). Burial and scour of truncated cones due to long-crested and short-crested nonlinear random waves. *Ocean System Engineering*, 4(1):21–37.

Myrhaug, D., Ong, M. C., Føien, H., Gjengedal, C., and Leira, B. J. (2009). Scour below pipelines and around vertical piles due to second-order random waves plus a current. *Ocean Engineering*, 36(8):605–616.

Myrhaug, D., Ong, M. C., and Gjengedal, C. (2008). Scour below marine pipelines in shoaling conditions for random waves. *Coastal Engineering*, 55(12):1219–1223.

Myrhaug, D. and Rue, H. (2003). Scour below pipelines and around vertical piles in random waves. *Coastal engineering*, 48(4):227–242.

Myrhaug, D. and Rue, H. (2005). Scour around group of slender vertical piles in random waves. *Applied Ocean Research*, 27(1):56–63.

Ping, F. (2013). Wave-induced scour below pipelines under shoaling random waves. *Master Project of NTNU*.

Roulund, A., Sumer, B. M., Fredsøe, J., and Michelsen, J. (2005). Numerical and experimental investigation of flow and scour around a circular pile. *Journal of Fluid Mechanics*, 534:351–401.

Sumer, B., Christiansen, N., Fredsoe, J., et al. (1992a). Time scale of scour around a vertical pile. In *The Second International Offshore and Polar Engineering Conference*. International Society of Offshore and Polar Engineers.

Sumer, B. M., Christiansen, N., and Fredsøe, J. (1993). Influence of cross section on wave scour around piles. *J. Waterway, Port, Coastal and Ocean Eng.*, 119(5):477–495.

Sumer, B. M., Christiansen, N., and Fredsøe, J. (1997). The horseshoe vortex and vortex shedding around a vertical wall-mounted cylinder exposed to waves. *Journal of Fluid Mechanics*, 332:41–70.

Sumer, B. M. and Fredsøe, J. (1990). Scour below pipelines in waves. *Journal of waterway, port, coastal, and ocean engineering*, 116(3):307–323.

Sumer, B. M. and Fredsøe, J. (1996). Scour around pipelines in combined waves and current. In *15th Conference on offshore mechanics and arctic engineering, OMAE*.

Sumer, B. M. and Fredsøe, J. (2000). Experimental study of 2d scour and its protection at a rubble-mound breakwater. *Coastal Engineering*, 40(1):59–87.

Sumer, B. M. and Fredsøe, J. (2001). Scour around pile in combined waves and current. *Journal of Hydraulic Engineering*, 127(5):403–411.

Sumer, B. M. and Fredsøe, J. (2002). *The mechanics of scour in the marine environment*. World Scientific.

Sumer, B. M., Fredsøe, J., and Christiansen, N. (1992b). Scour around vertical pile in waves. *Journal of waterway, port, coastal, and ocean engineering*, 118(1):15–31.

Young, I. R. (1999). *Wind generated ocean waves*, volume 2. Elsevier.

Appendix A

The Battjes and Groenendijk (2000) truncated probability density function of $\hat{H}$ is given by

1) Waves alone case

$$f_{\widehat{H}} = \begin{cases} p_1(\hat{H}) = \frac{k_1}{\hat{H}}(\frac{\hat{H}}{\hat{H}_1})^{k_1} \exp\left[-\left(\frac{\hat{H}}{\hat{H}_1}\right)^{k_1} + \left(\frac{\hat{H}_t}{\hat{H}_1}\right)^{k_1}\right], & \hat{H}_t \leq \hat{H} \leq \hat{H}_{tr} \\ \\ p_2(\hat{H}) = \frac{k_2}{\hat{H}}(\frac{\hat{H}}{\hat{H}_2})^{k_2} \exp\left[-\left(\frac{\hat{H}}{\hat{H}_2}\right)^{k_2} + \left(\frac{\hat{H}_t}{\hat{H}_2}\right)^{k_2}\right], & \hat{H} \geq \hat{H}_{tr} \end{cases} \tag{A.1}$$

2) Waves plus current

$$f_{\widehat{H}} = \begin{cases} p_1(\hat{H}) = (\frac{k_1}{\hat{H}}(\frac{\hat{H}}{\hat{H}_1})^{k_1} + 4.7k_1(\frac{\hat{H}_t}{\hat{H}_1})^{k_1}\frac{\hat{U}_c}{(U_c+\hat{H})^2} \exp\left[-\left(\frac{\hat{H}}{\hat{H}_1}\right)^{k_1} + \left(\frac{\hat{H}_t}{\hat{H}_1}\right)^{k_1}\right], & \hat{H}_t \leq \hat{H} \leq \hat{H}_{tr} \\ \\ p_2(\hat{H}) = (\frac{k_2}{\hat{H}}(\frac{\hat{H}}{\hat{H}_2})^{k_2} + 4.7k_2(\frac{\hat{H}_t}{\hat{H}_2})^{k_2}\frac{\hat{U}_c}{(U_c+\hat{H})^2} \exp\left[-\left(\frac{\hat{H}}{\hat{H}_1}\right)^{k_1} + \left(\frac{\hat{H}_t}{\hat{H}_2}\right)^{k_2}\right], & \hat{H} \geq \hat{H}_{tr} \end{cases} \tag{A.2}$$

The Battjes and Groenendijk (2000) probability density function of $\hat{H}$ is given by

$$f_{\widehat{H}} = \begin{cases} p_1(\hat{H}) = \frac{k_1}{\hat{H}}(\frac{\hat{H}}{\hat{H}_1})^{k_1} \exp\left[-\left(\frac{\hat{H}}{\hat{H}_1}\right)^{k_1}\right], & \hat{H} \leq \hat{H}_{tr} \\ \\ p_2(\hat{H}) = \frac{k_2}{\hat{H}}(\frac{\hat{H}}{\hat{H}_2})^{k_2} \exp\left[-\left(\frac{\hat{H}}{\hat{H}_2}\right)^{k_2}\right], & \hat{H} \geq \hat{H}_{tr} \end{cases} \tag{A.3}$$

Appendix B

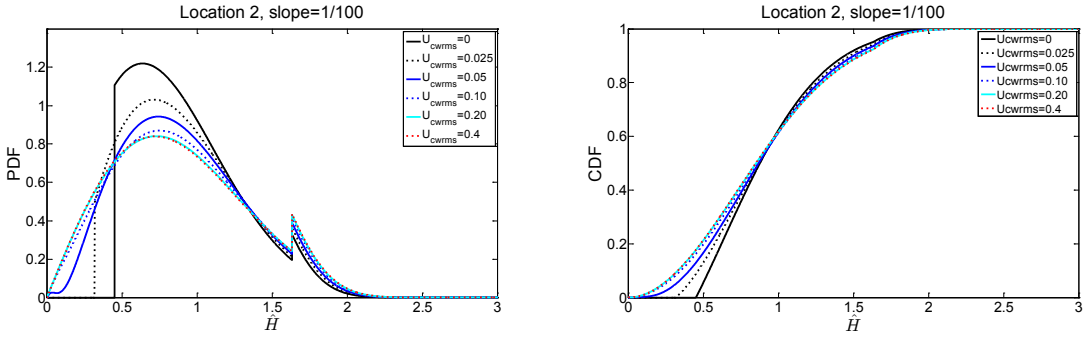

(a) PDF (b) CDF

Fig. B.1 Truncated wave height distribution at Location 2 for scour around a vertical pile

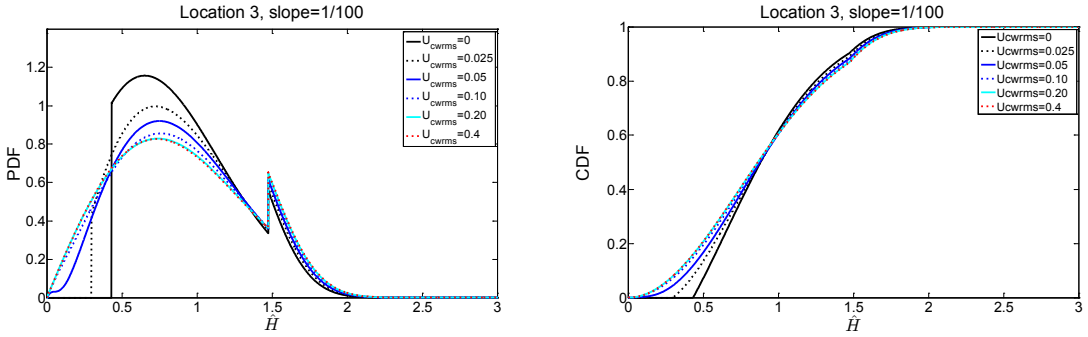

(a) PDF (b) CDF

Fig. B.2 Truncated wave height distribution at Location 3 for scour around a vertical pile

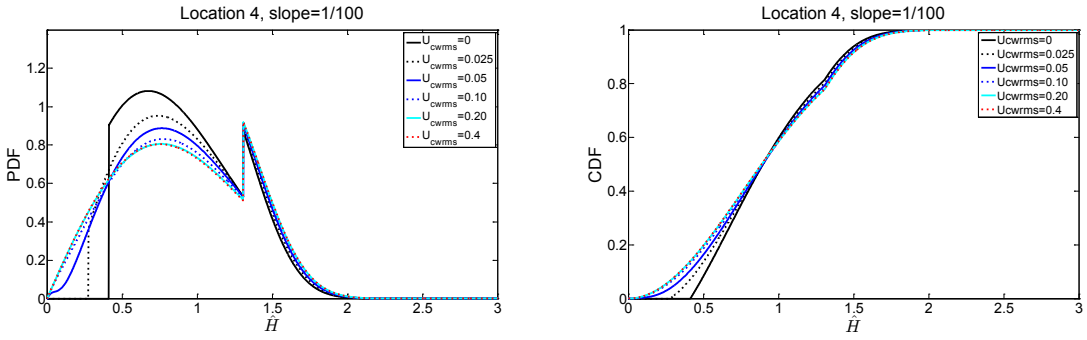

(a) PDF (b) CDF

Fig. B.3 Truncated wave height distribution at Location 4 for scour around a vertical pile